分光観測と物理情報

定金　晃三（大阪教育大学）

当日配布した資料を再録しました.

なお，P.3 は欠となっています.

Spectroscopic Astrophysics

From the Sun to QSOs

The Sun

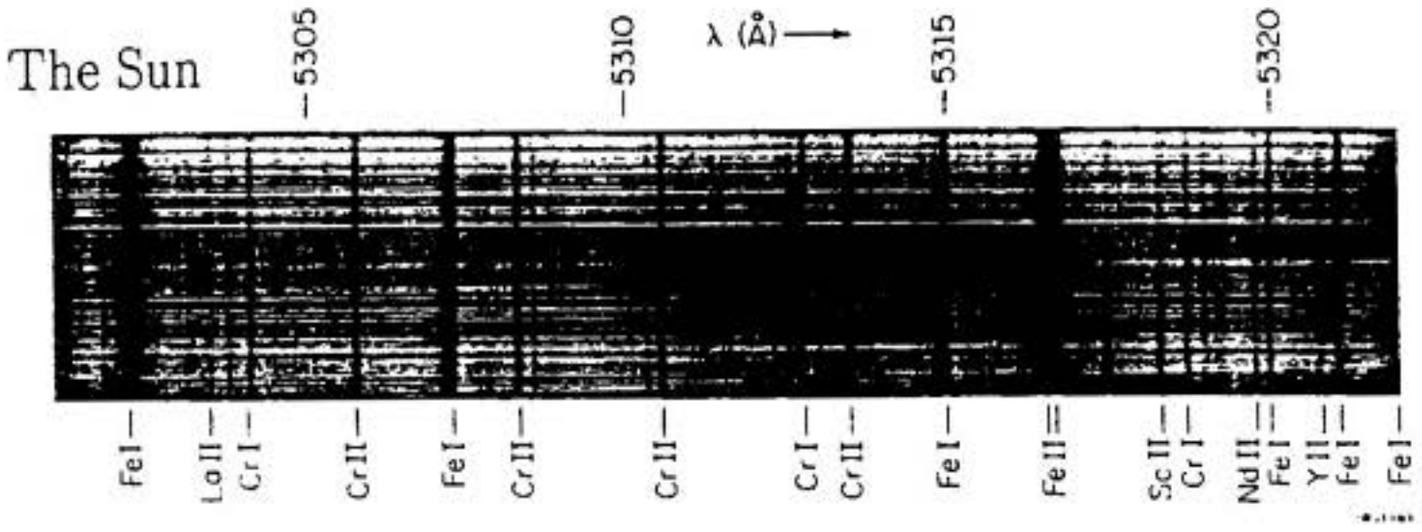

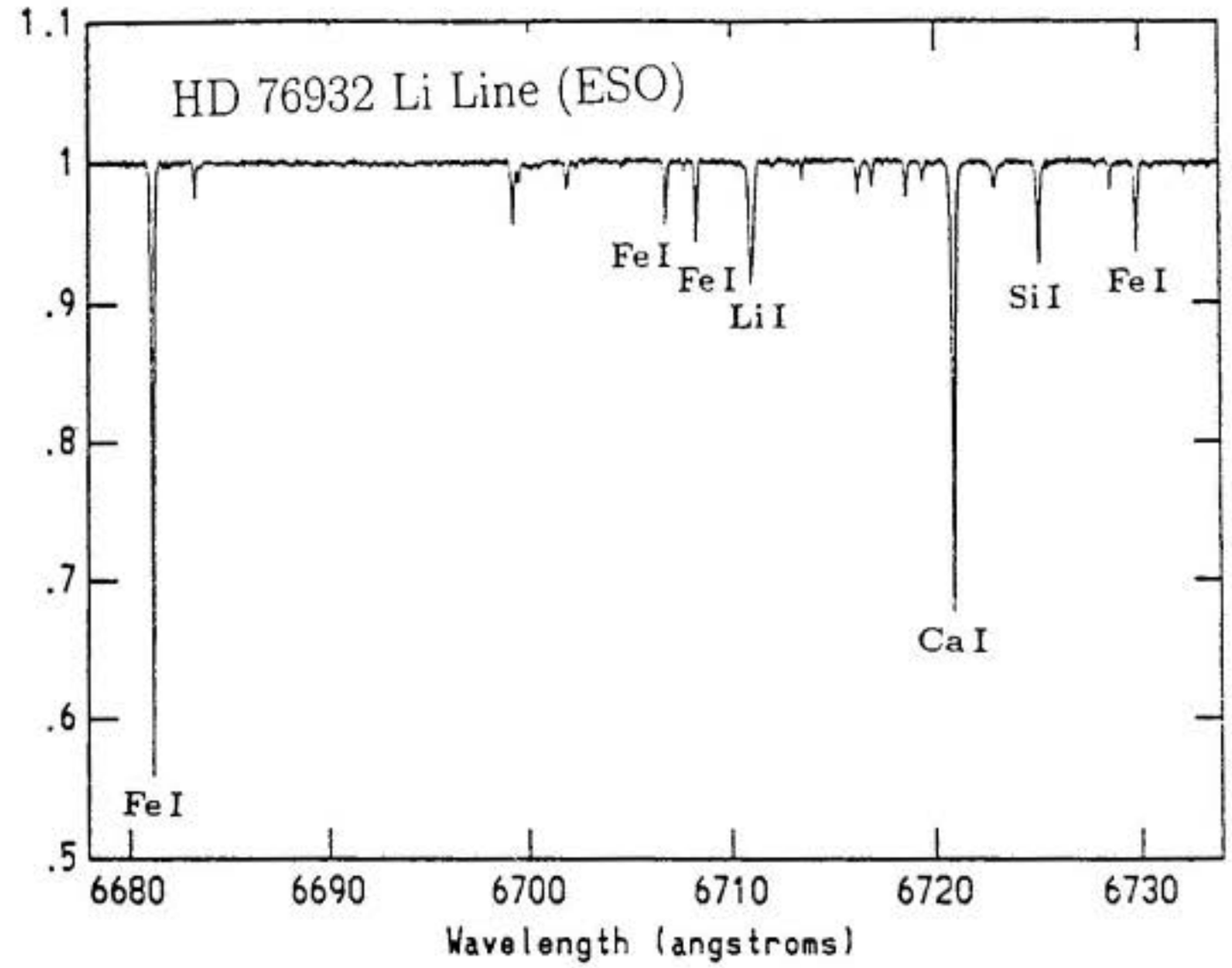

LMC O-Star UV (HST)

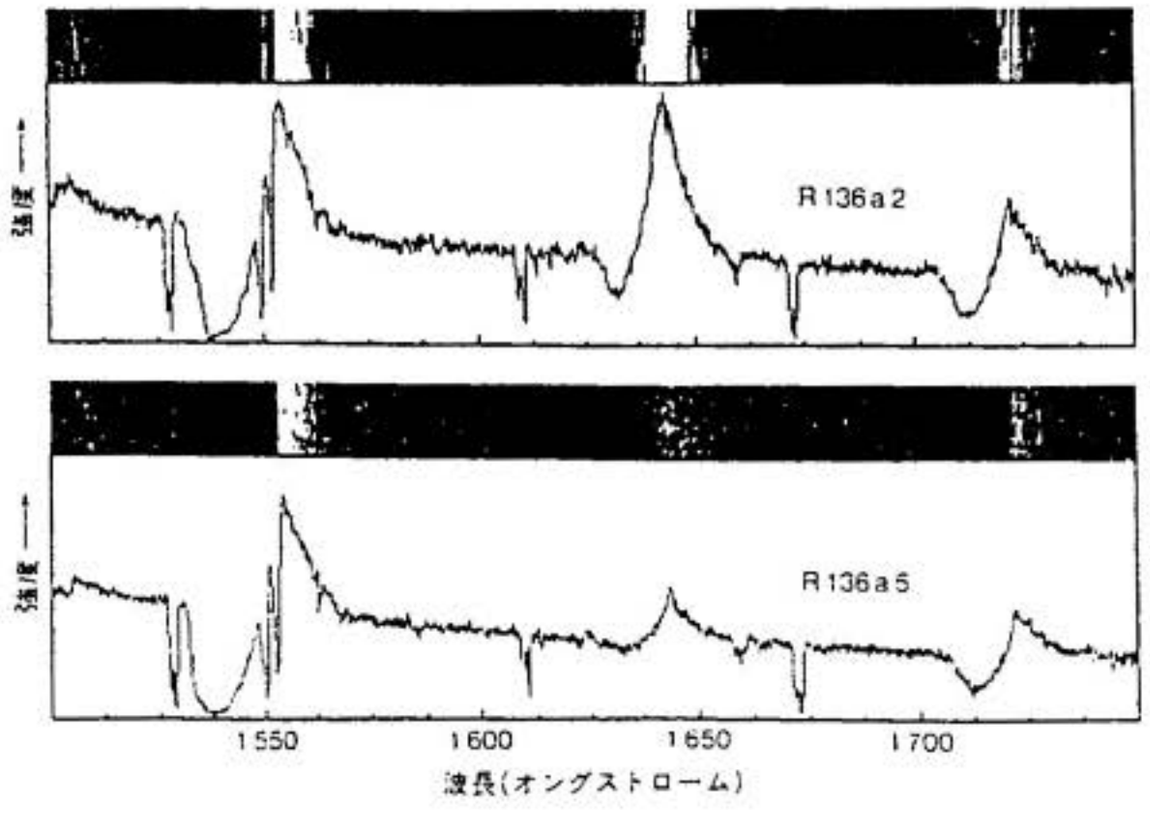

QSO HS 1946+7658 (Okayama)

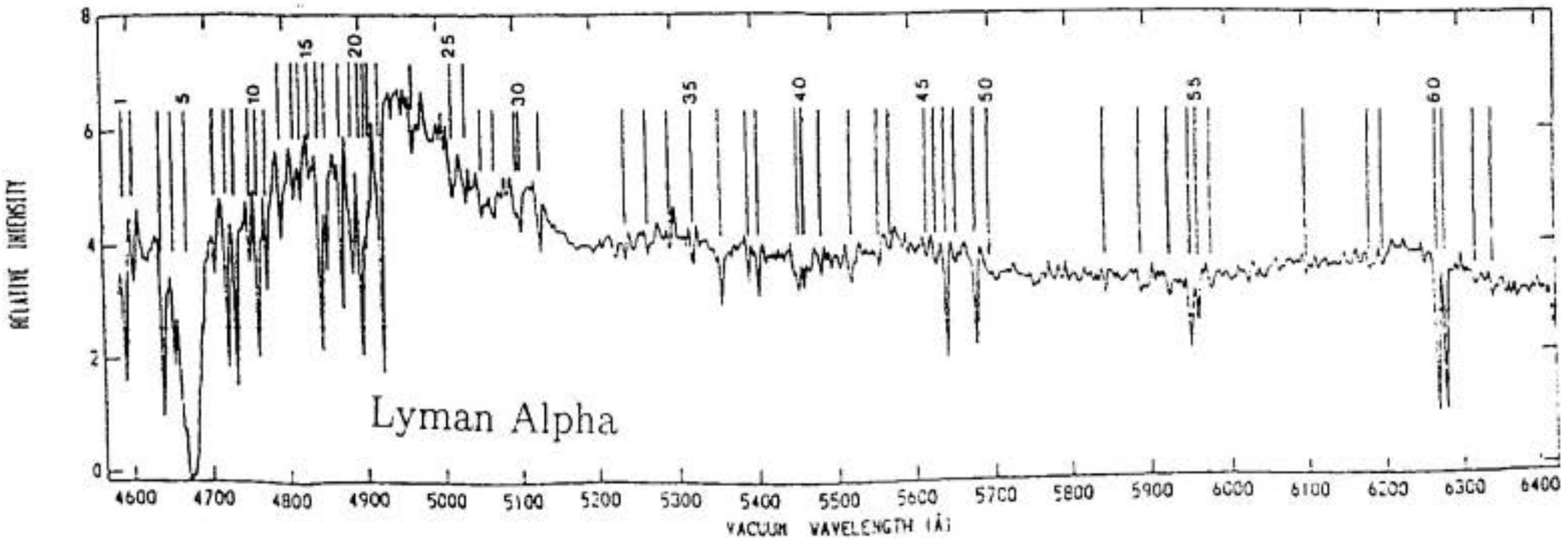

Spectrograph
分光器

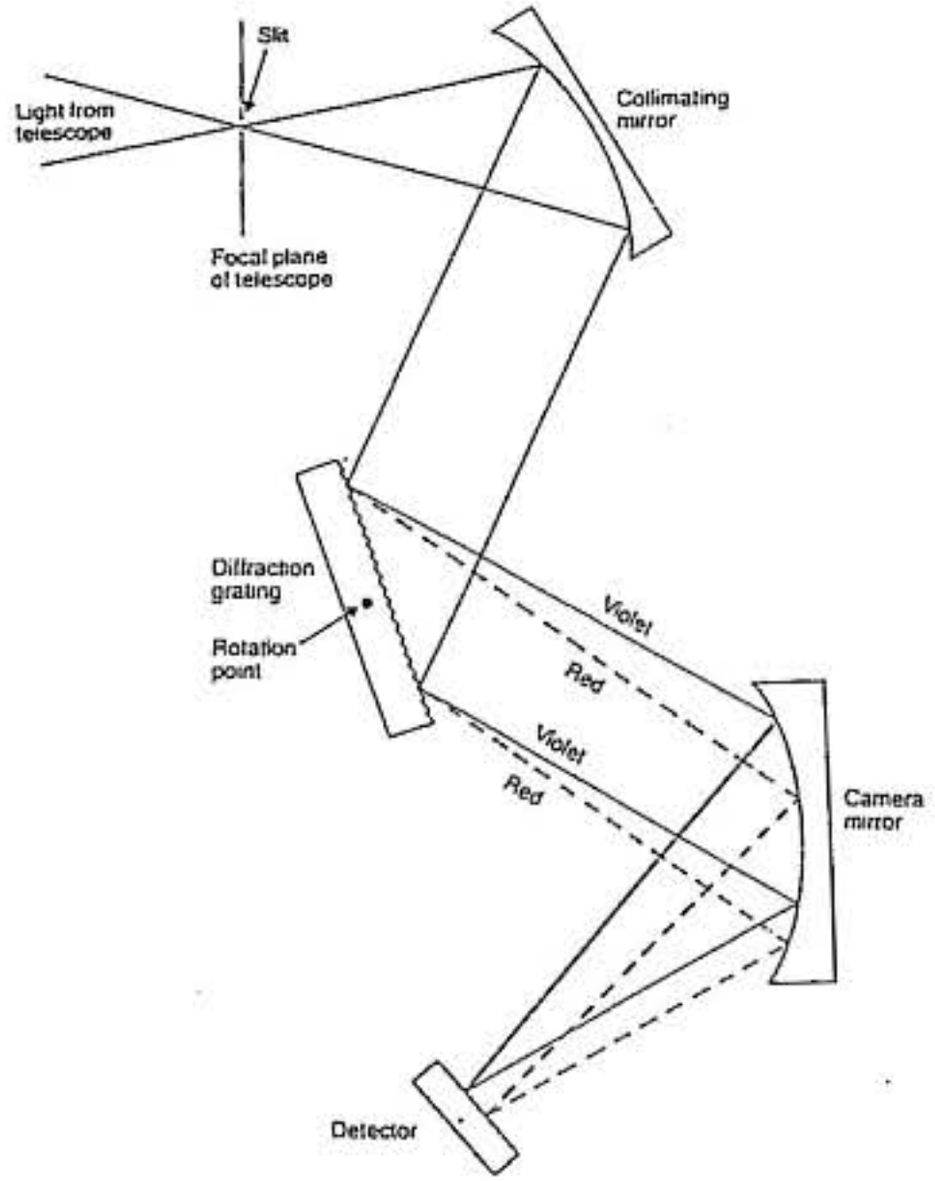

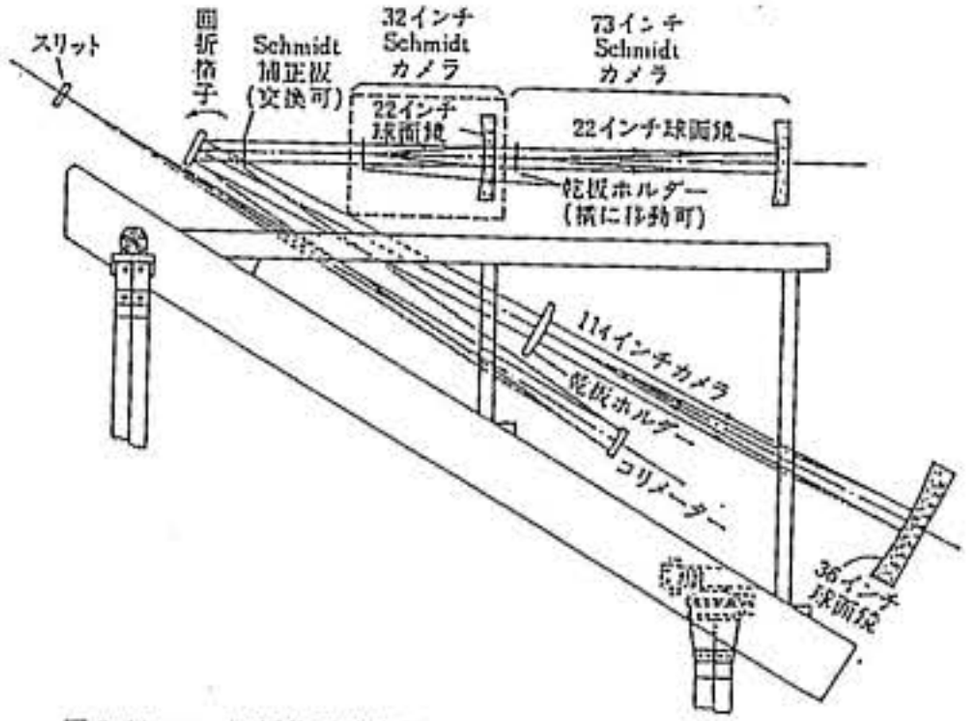

図 9.11 a-c　回折格子分光器
a) 回折格子の働き(溝格子) 隣り合う光束の光路差が $d(\sin\alpha - \sin\beta) = n\lambda$ ($n = \pm1, \pm2, \cdots$; d=格子定数)になると干渉縞の極強点，つまりスペクトル線が生じる．分散度(Å/mm)や分解能は他の条件が同じなら'次数' n が大きくなるにつれて比例的に高まる． b) 格子溝または格子段における特定の入射・出射角の光束に対しては鏡面反射の条件が成り立ち(いわゆる'ブレーズ')，格子にアルミニウムなどを蒸着するとその方向の近くのスペクトルは格段と明るくなる． c) ウィルソン山天文台の Coudé 分光器　100インチ望遠鏡の Coudé 系は分光器のスリット上に星像を結ばせる．コリメーターは光束を平行にして格子に送る．スペクトルに分解された光は相互に交換可能な 114 インチ，73 インチまたは 32 インチ Schmidt カメラの焦点で結像する．(16 インチと 8 インチカメラはここには描いてない．) 格子が同時にカメラの入射絞りとなっている．補正板は大きな口径比をもった短焦点のカメラにだけ必要である．

ウィルソン
100インチ
クーデ

エシェル
分光器

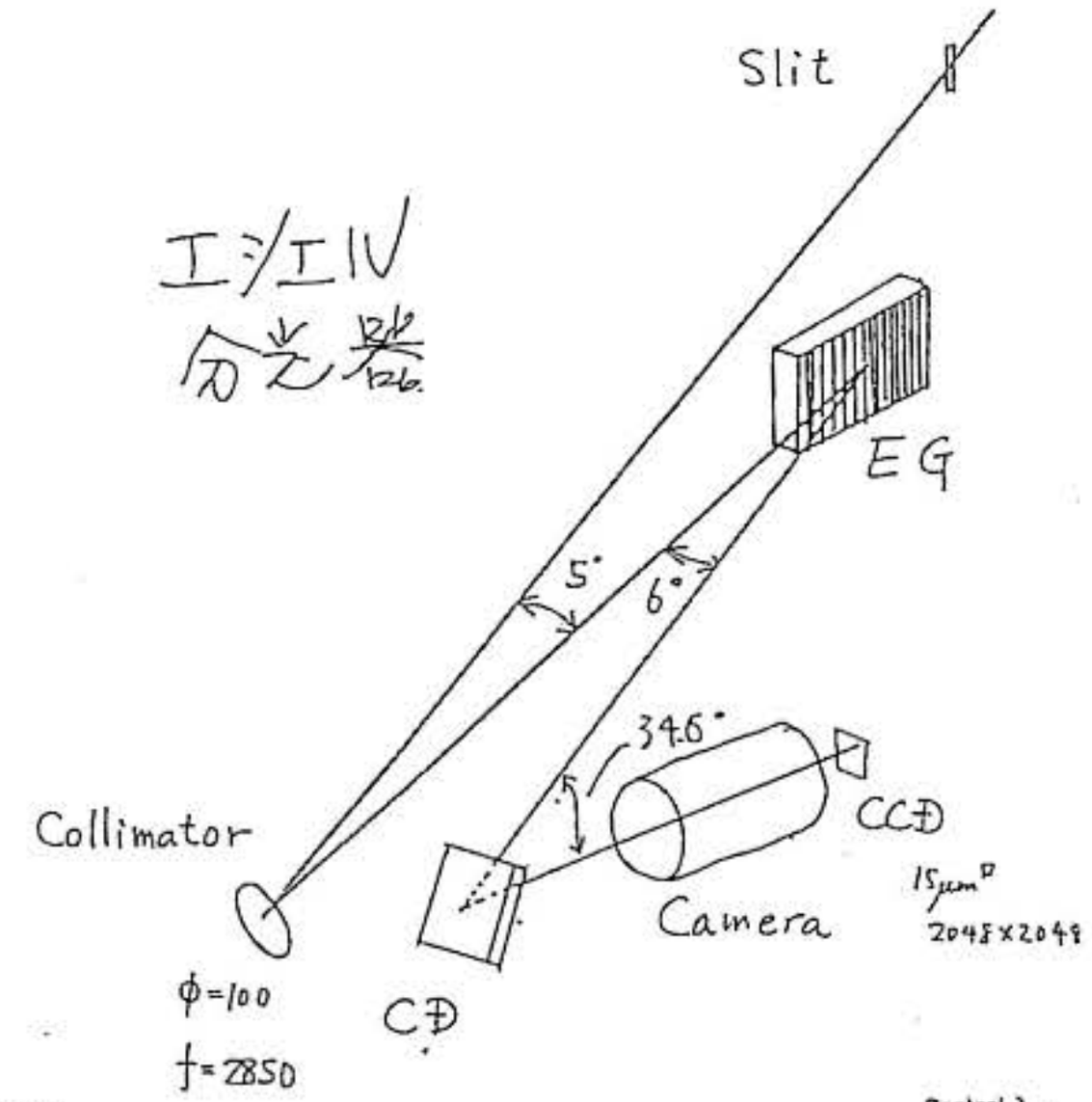

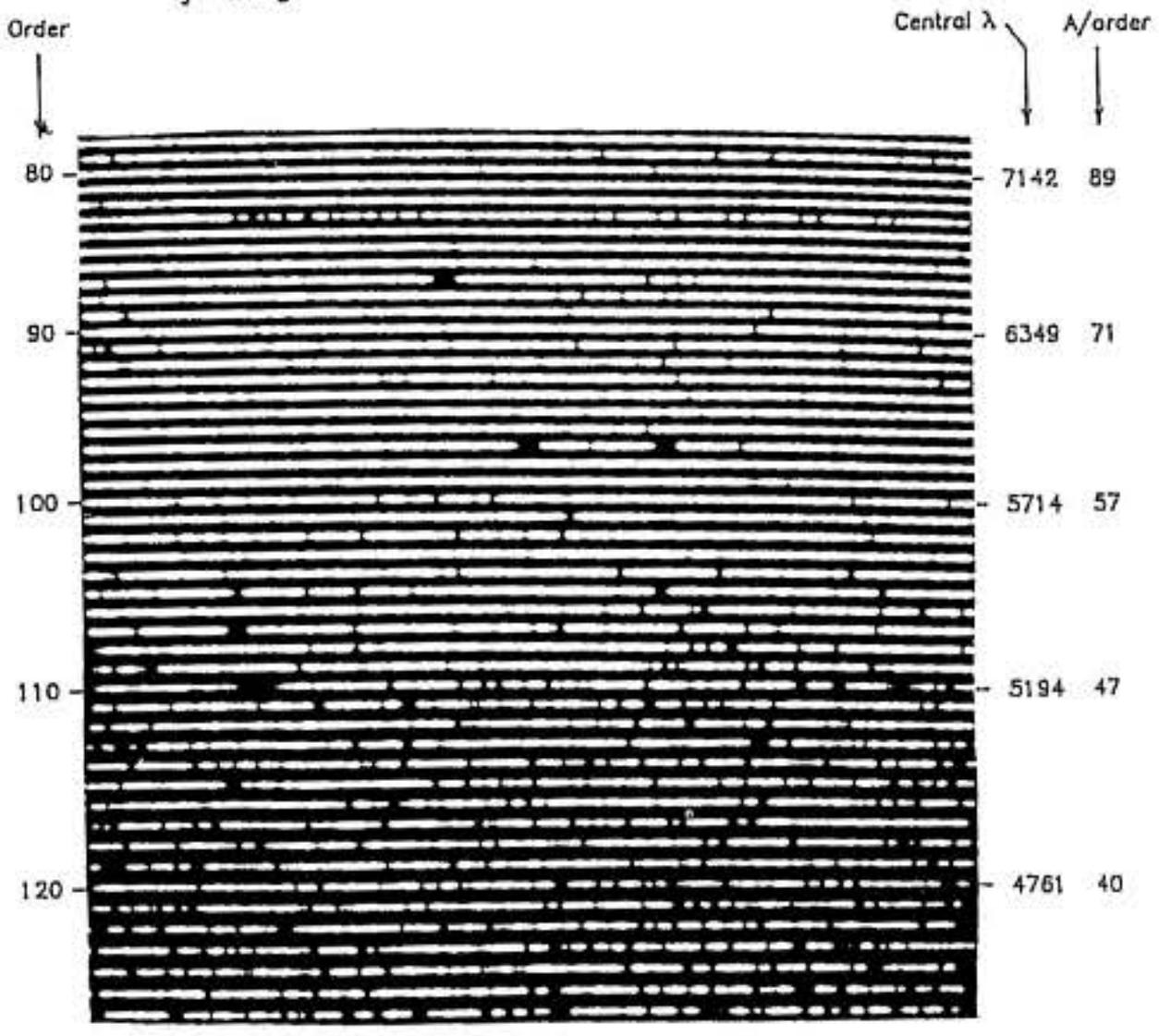

Fig. 3.20. This echellogram shows the central portions of 49 orders spanning a range of wavelength from 4500 Å to 7300 Å. The field is limited by the size of the detector. The full coverage by the spectrograph is 3600 Å to 9500 Å. The resolving power is 30000, and the star (A4, V = 12.3) is in the globular cluster M71. The strong line in order 87 is H_γ, and the two in order 97 are the sodium D lines. Details can be seen in Vogt (1987). (Photograph courtesy of S.S. Vogt)

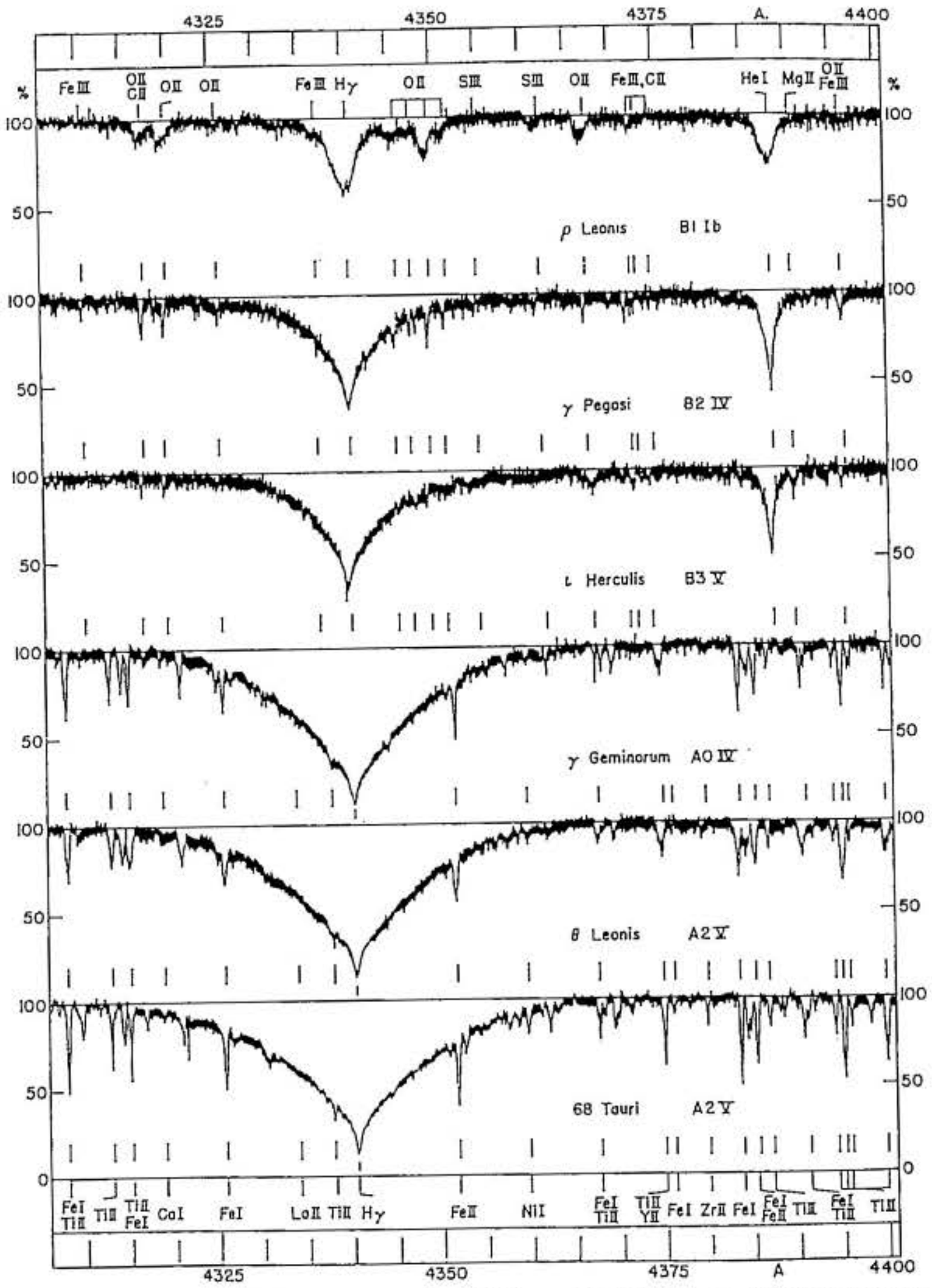

Figure 2-1.2 Intensity tracings of the spectra shown in Figure (2-1.1) [*courtesy* K.O.Wright, Dominion Astrophysical Observatory]

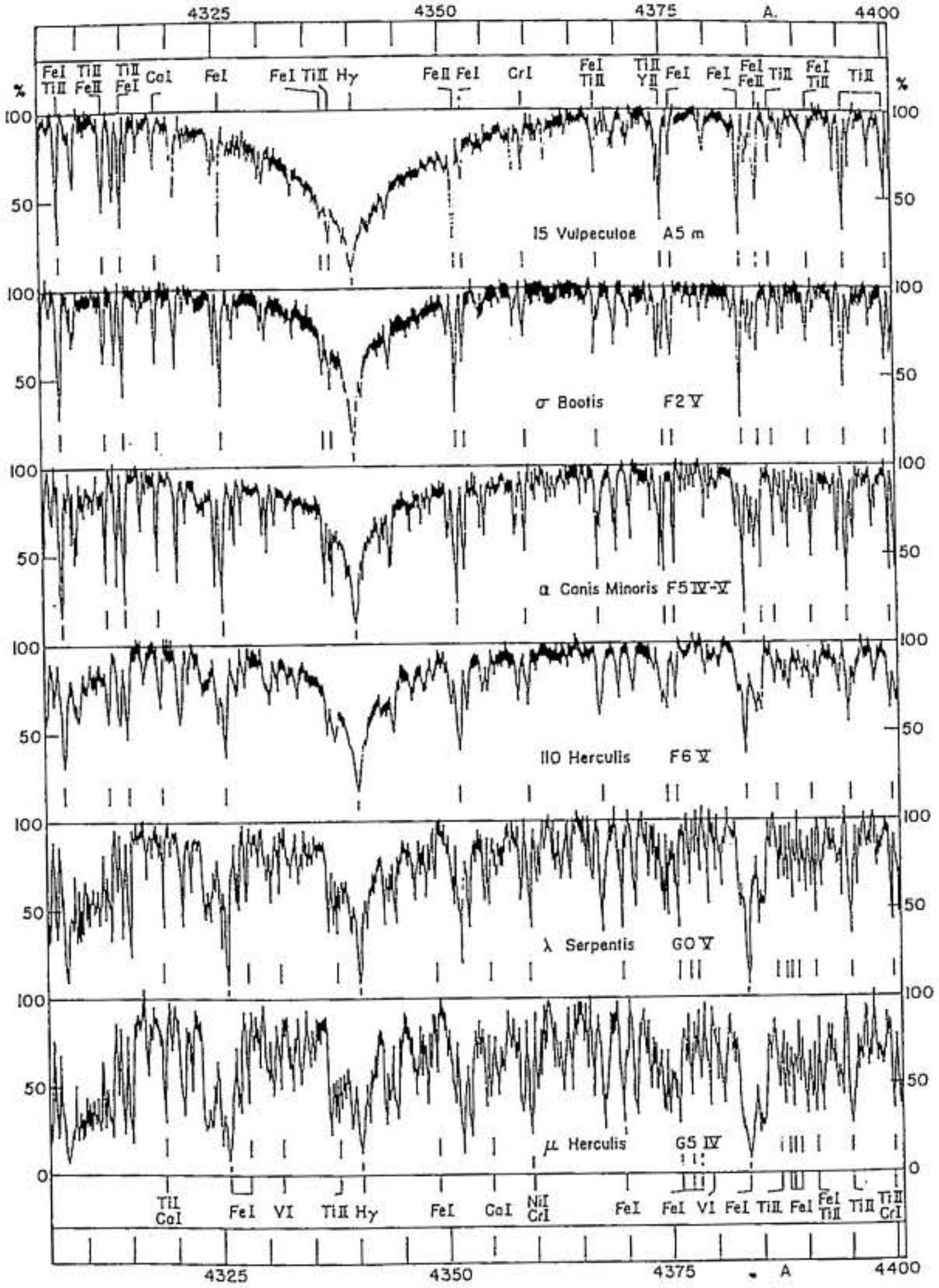

Figure 2-1.3 Intensity tracings of the spectra shown in Figure (2-1.1), *continued* [*courtesy* K.O.Wright, Dominion Astrophysical Observatory]

Line Spectra

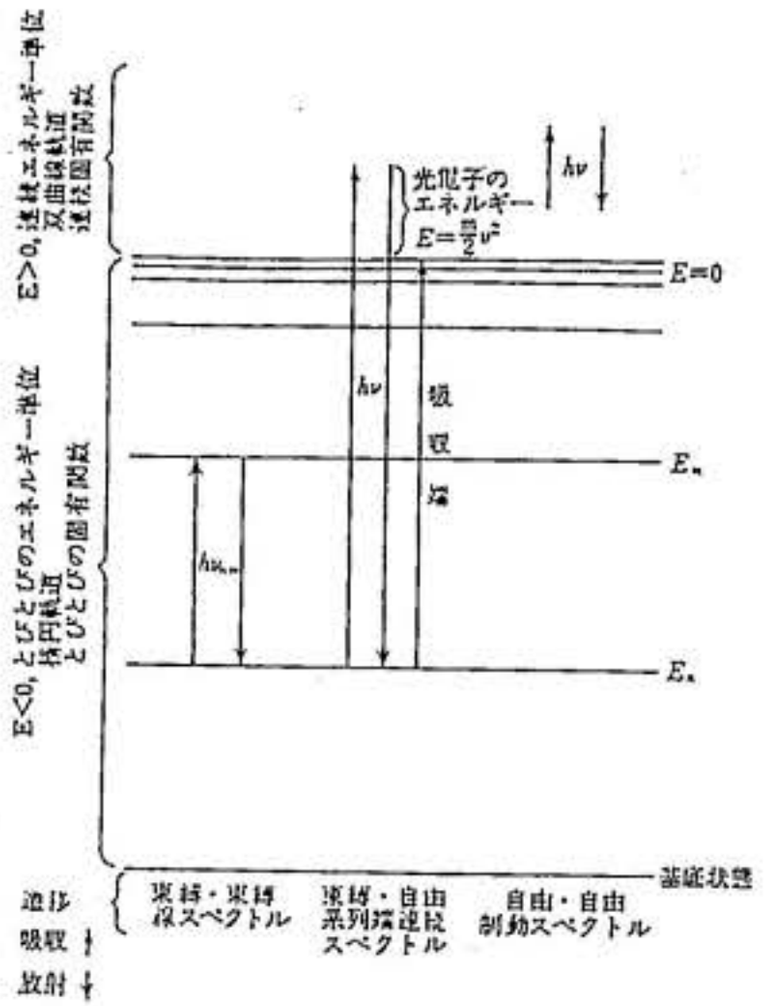

図 17.1 原子のエネルギー単位図表(Grotrian 図表)と遷移(模式化してある)

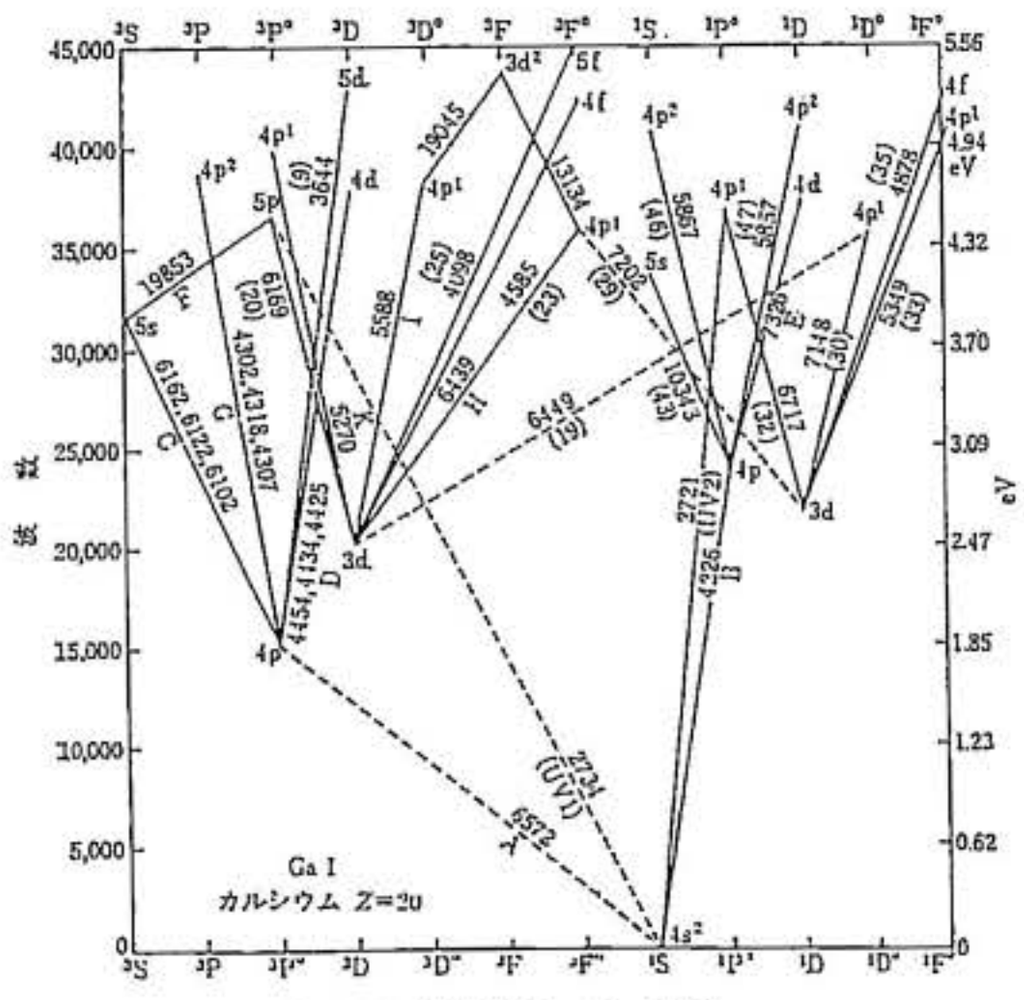

図 17.3 項位図表(Grotrian 図表)
中性カルシウム Ca I の(遠強)スペクトルのもの.

RMT (The Revised Multiplet Table)
C. H. Moore, 1959, NBS

Ca I	I P 6.09	Anal A	List B	Mar. 1944	
6572.781	A	50	0.00 1.88	0-1	$4^1S-4^3P^\circ$ (1)
4226.738//	A	500R	0.00 2.93	0-1	$4^1S-4^1P^\circ$ (2)
6162.173	A	150	1.89 3.89	2-1	$4^3P^\circ-5^3S$
6122.219	A	100	1.88 3.89	1-1	(3)
6102.723	A	80	1.87 3.89	0-1	
4454.781	A	80	1.89 4.66	2-3	$4^3P^\circ-4^3D$
4434.960	A	60r	1.88 4.66	1-2	(4)
4425.441	A	50	1.87 4.66	0-1	
4455.887	A	40	1.89 4.66	2-2	
4435.688	A	40	1.88 4.66	1-1	
4456.613	B	10	1.89 4.66	2-1	
4302.527	A	60r	1.89 4.76	2-2	$4^3P^\circ-4p^2\ 3P$
4298.986	A	(30)	1.88 4.75	1-1	(5)
4318.653	A	45	1.89 4.75	2-1	r
4307.741	A	45	1.88 4.74	1-0	
4283.010	A	40	1.88 4.76	1-2	
4289.364	A	40	1.87 4.75	0-1	
3973.707	A	12	1.89 5.00	2-1	$4^3P^\circ-6^3S$
3957.053	A	10	1.88 5.00	1-1	(6)
3948.901	A	6	1.87 5.00	0-1	
3933.50	D	(0)	1.88 5.02	1-0	$4^3P^\circ-4p^2\ 1S$ (7)
3761.73	E	(0)	1.88 5.16	1-0	$4^3P^\circ-6^1S$ (8)
3644.410	A	40	1.89 5.28	2-3	$4^3P^\circ-5^3D$
3630.748	A	30	1.88 5.28	1-2	(9)
3624.111	A	20	1.87 5.28	0-1	
3644.765	A	15	1.89 5.28	2-2	
3630.974	A	15	1.88 5.28	1-1	
3644.990	B	2	1.89 5.28	2-1	
3487.598	A	12	1.89 5.43	2-1	$4^3P^\circ-7^3S$
3474.763	A	8	1.88 5.43	1-1	(10)
3468.476	A	4	1.87 5.43	0-1	
3361.918	A	35n*	1.89 5.58	2-3	$4^3P^\circ-8^3D$
3350.209	A	25n*	1.88 5.58	1-2	(11)
3344.513	A	8n	1.87 5.56	0-1	
3362.131	B	35n*	1.89 5.56	2-2	
3350.361	B	25n*	1.88 5.58	1-1	
3362.28	B	(0)	1.89 5.56	2-1	
3288.067	A	4	1.89 5.65	2-1	$4^3P^\circ-8^3S$
3274.661	B	2	1.88 5.65	1-1	(12)
3269.090	B	1n	1.87 5.65	0-1	
3225.896	A	8n*	1.89 5.72	2-3	$4^3P^\circ-7^3D$
3215.145	B	5n*	1.88 5.72	1-2	(13)
3209.830	B	2n	1.87 5.72	0-1	
3228.129	B	8n*	1.89 5.72	2-3	
3215.334	B	5n*	1.88 5.72	1-1	

The Solar Spectrum
Mt. Wilson

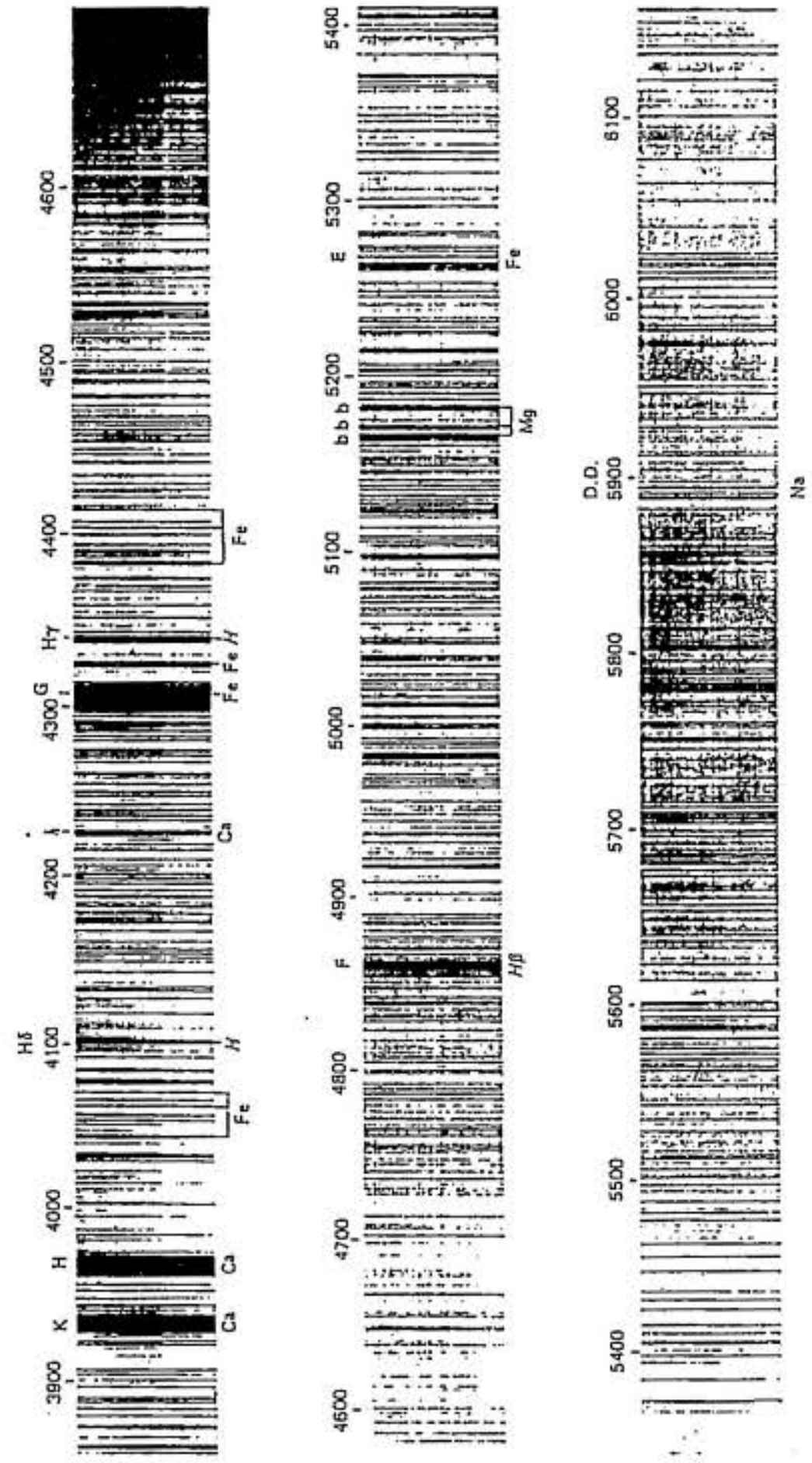

Spectral Information I Line Identification

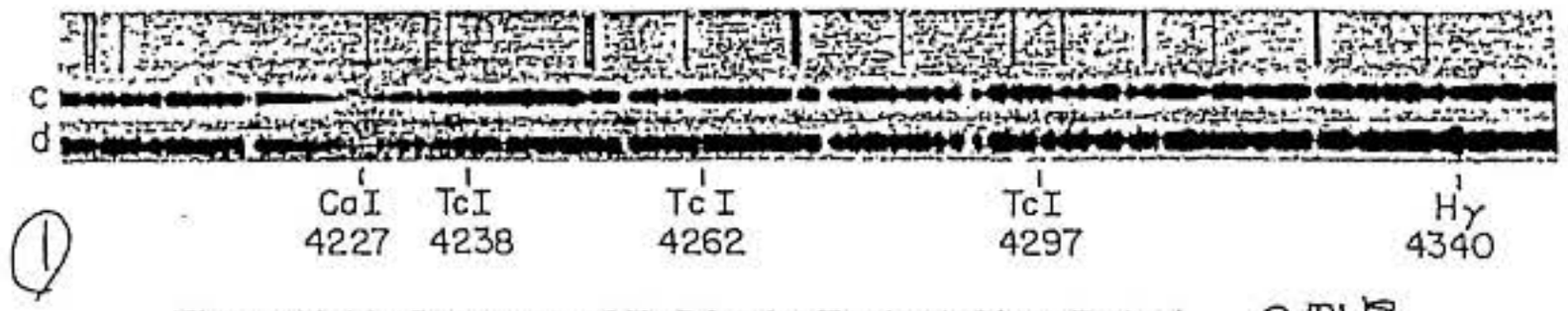

① Figure 13.10. Spectrum of Tc I in the Evolved·Giant R And. S型星

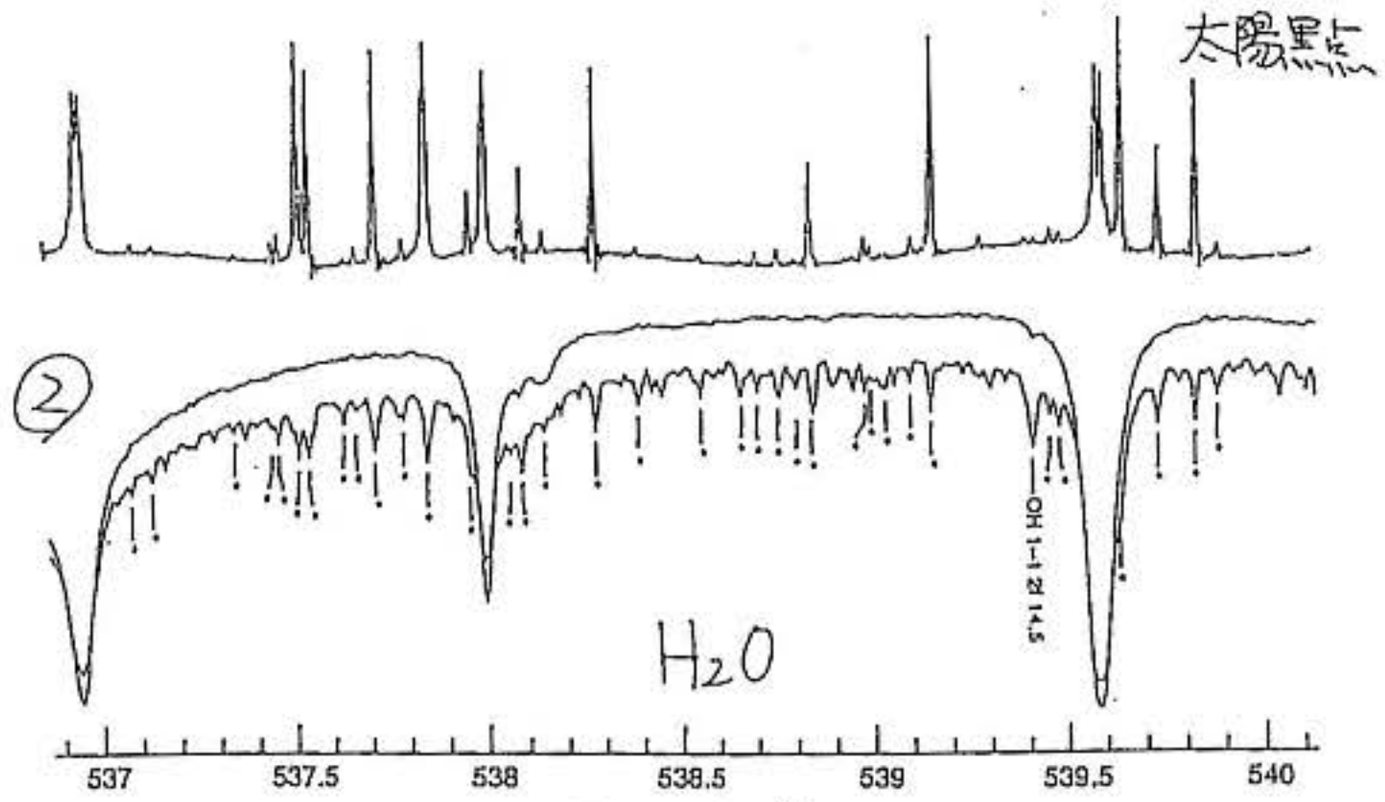

g. 4. A comparison between the laboratory emission spectrum (top trace) of hot water, the spectrum a sunspot penumbra (middle trace), and a sunspot umbra (lower trace) (water peaks are indicated by). The water features at 537 cm^{-1} and 539.6 cm^{-1} show self-absorption in the laboratory emission pectrum and correspond to telluric water features in the lower two traces.

多胡-佐藤-小坂彗星 1969

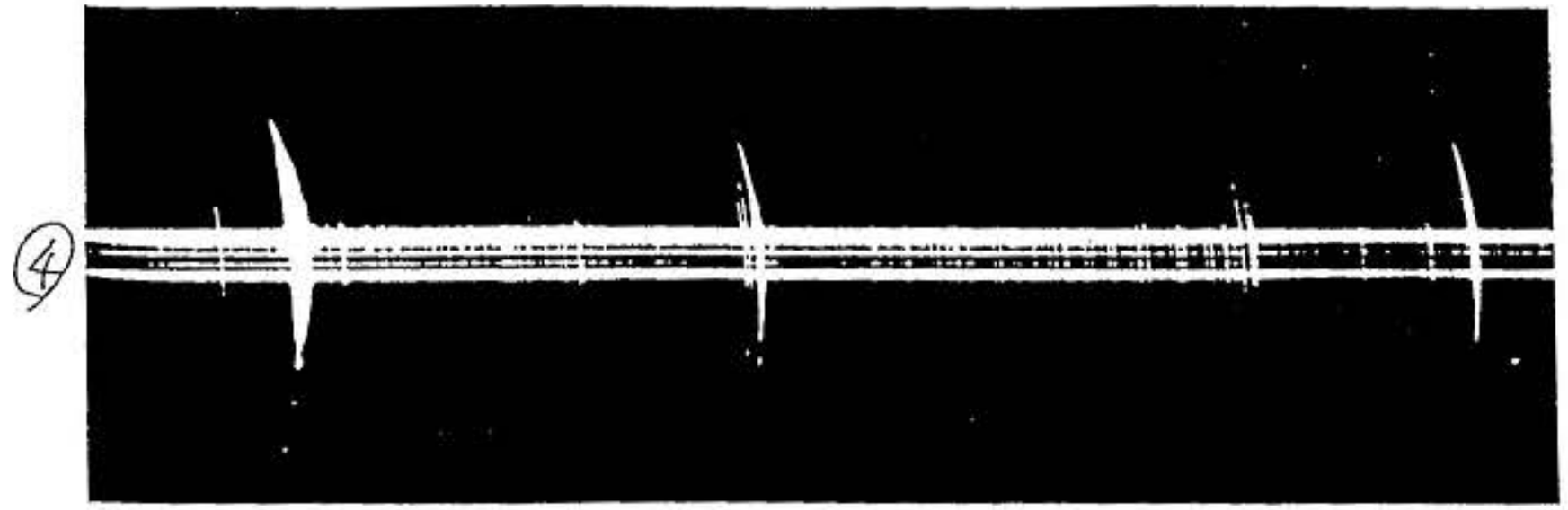

太陽彩層 フラッシュ・スペクトル

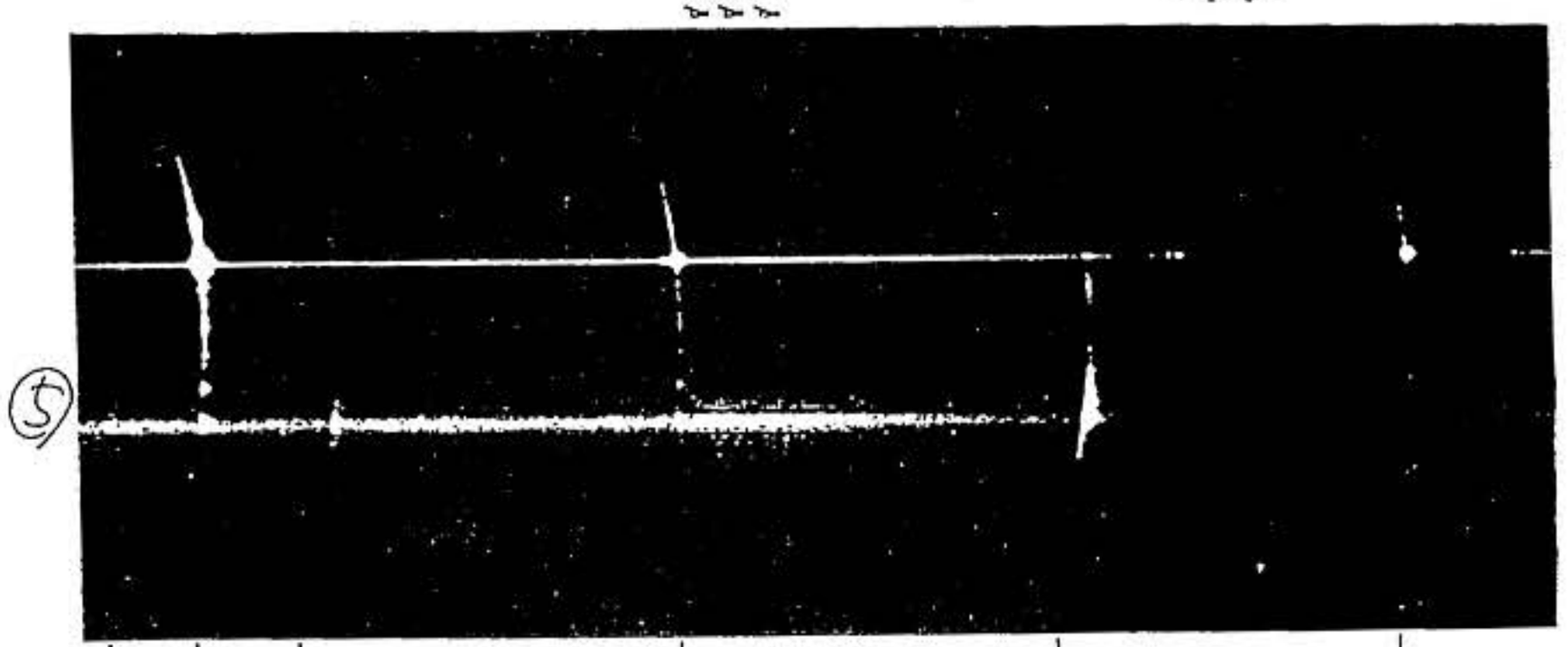

コロナ輝線

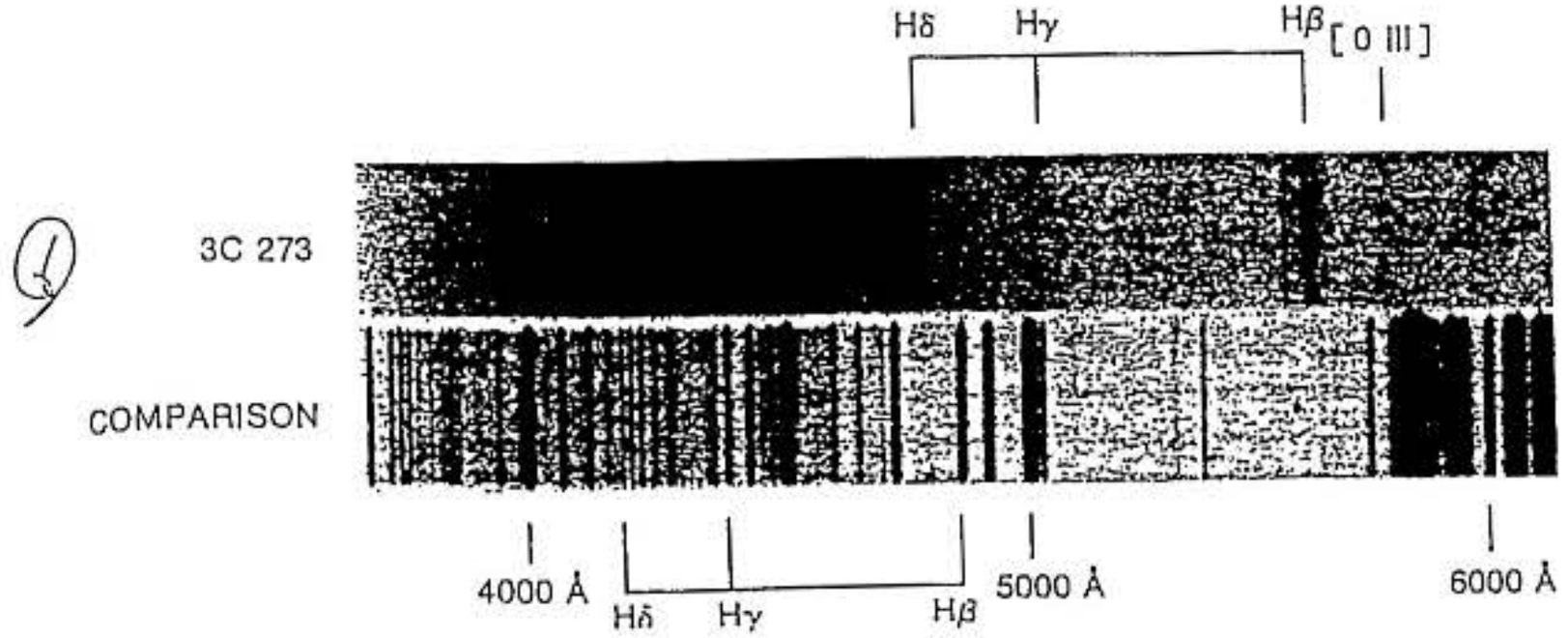

Spectral Information II Radial Velocity.

o Spectroscopic Binary

1

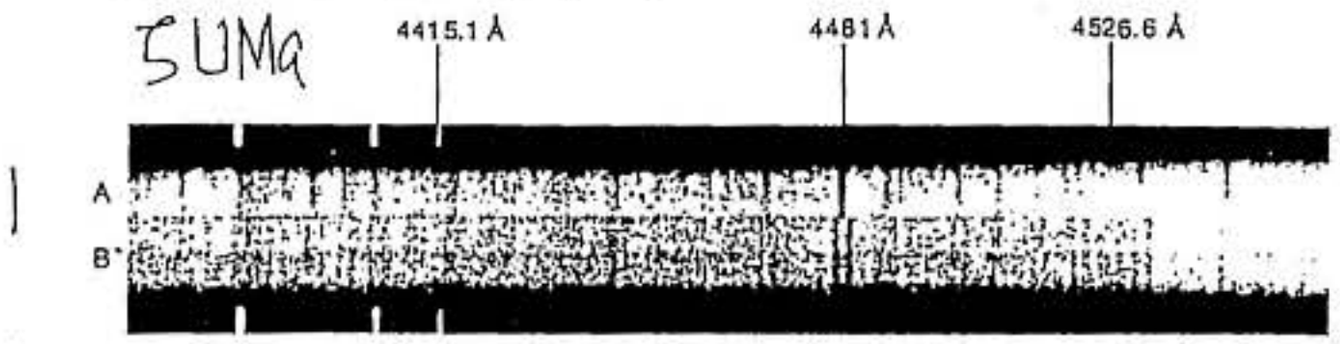

2

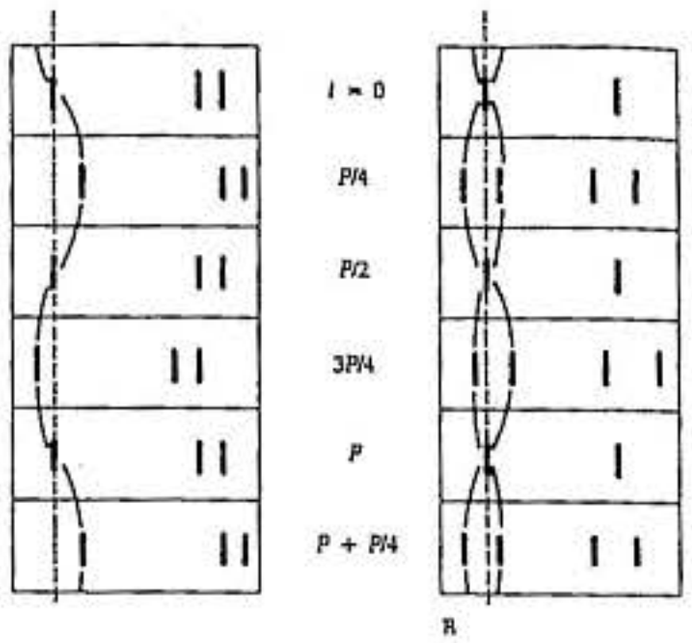

3

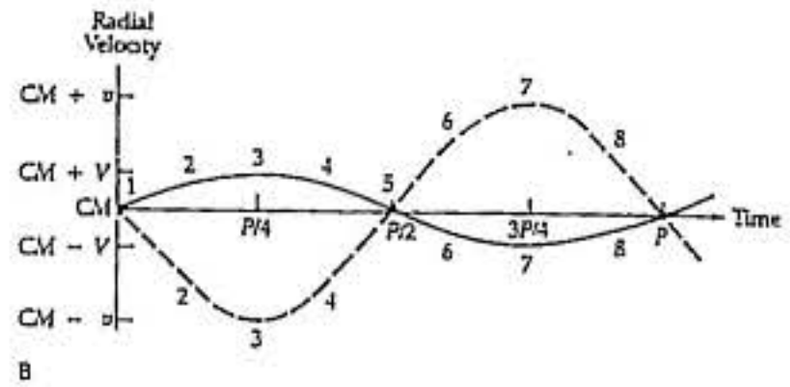

4

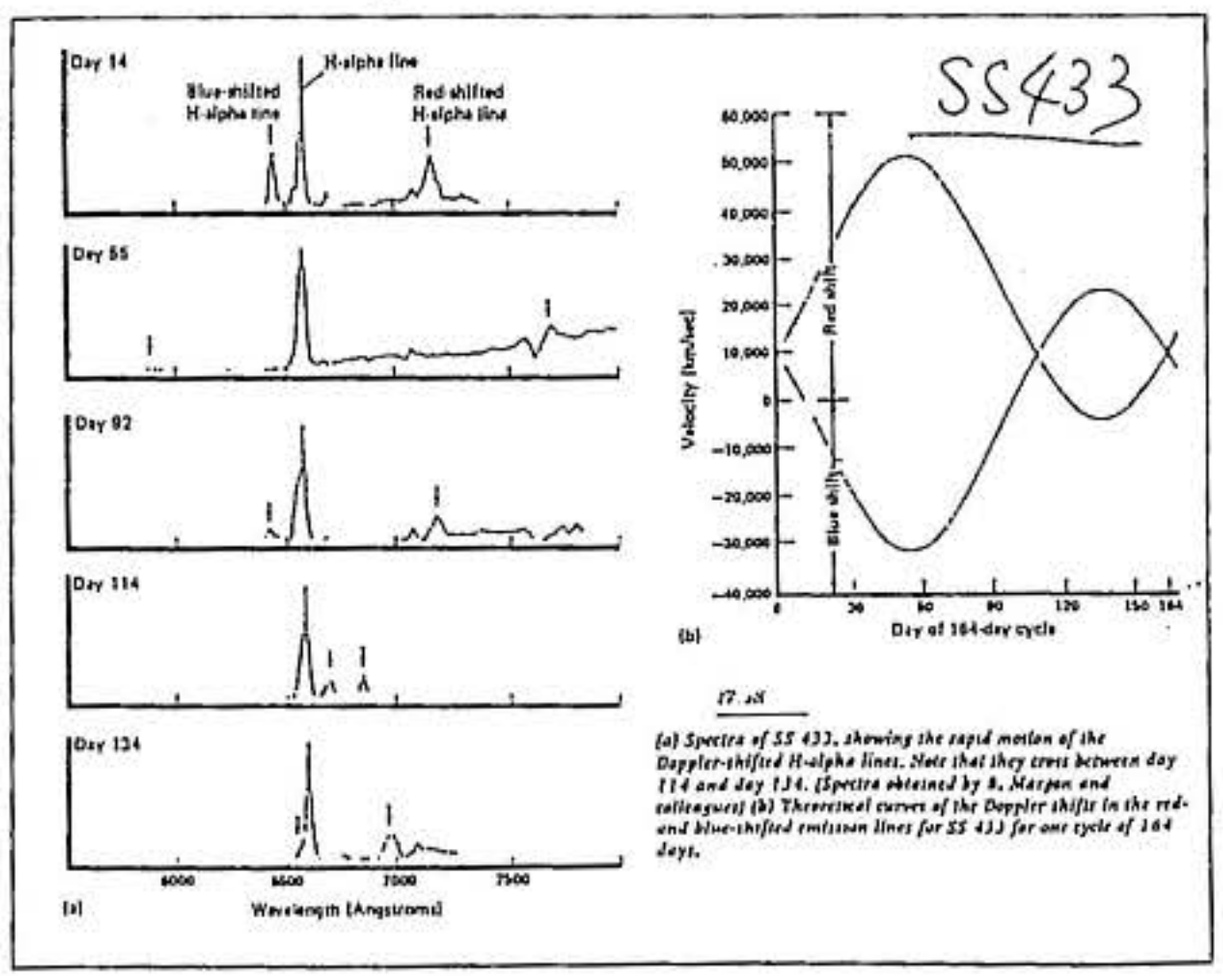

(a) Spectra of SS 433, showing the rapid motion of the Doppler-shifted H-alpha lines. Note that they cross between day 114 and day 134. (Spectra obtained by B. Margon and colleagues) (b) Theoretical curves of the Doppler shift in the red- and blue-shifted emission lines for SS 433 for one cycle of 164 days.

High precision Radial Velocity.

5

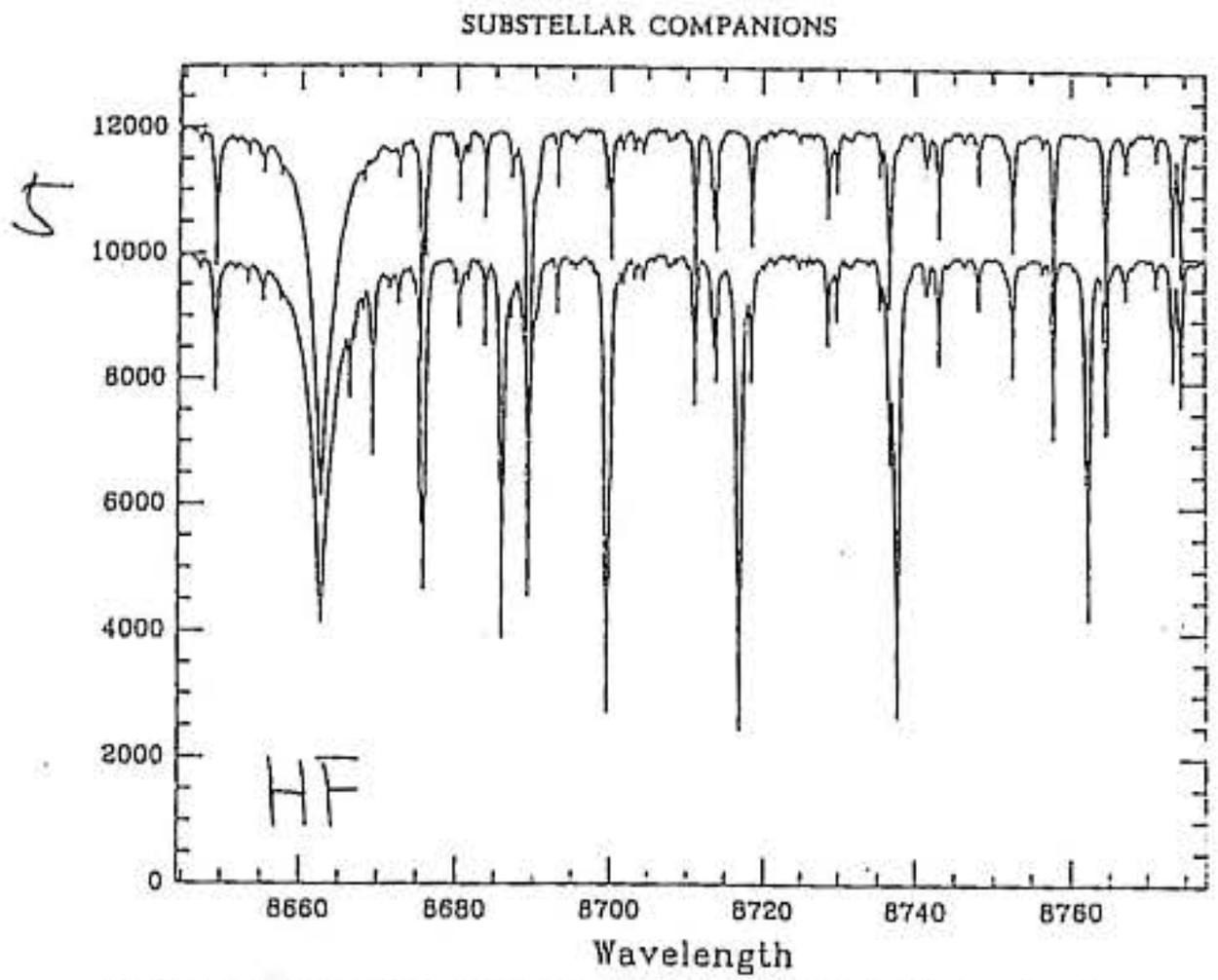

FIG. 1.—Spectra of 61 Cyg A with (*lower*) and without (*upper*) the *R* branch of the 3–0 band of hydrogen fluoride superposed

6

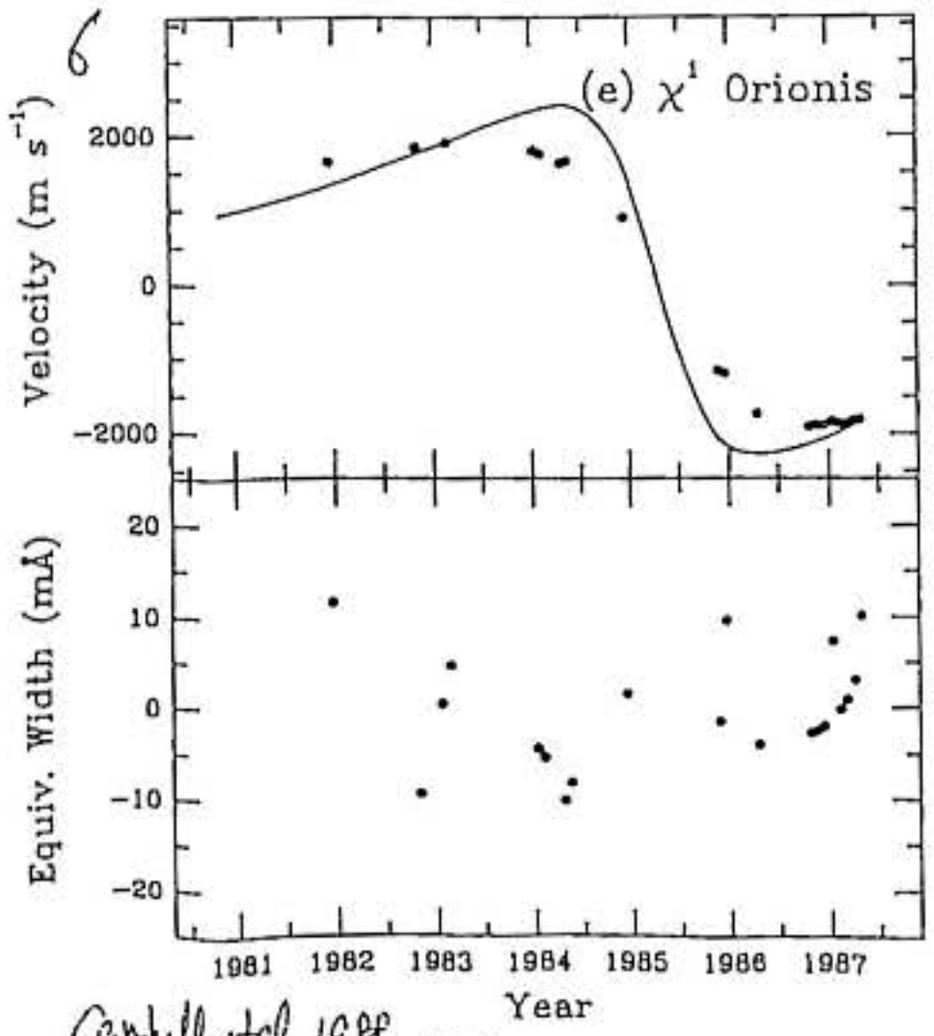

Cantell et al. 1988
A.P.J. 331, 961

FIG. 2e

7

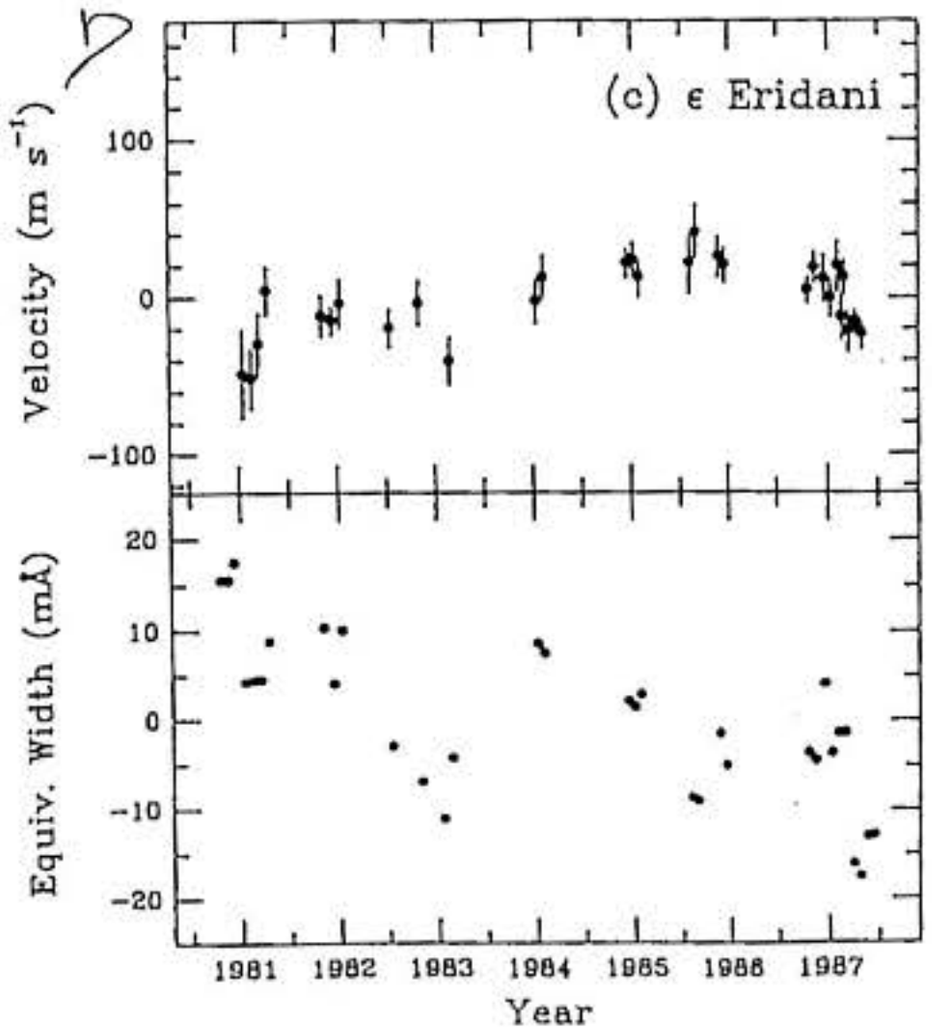

FIG. 2c

Spectral Information III Line profiles

Stellar Rotation

1

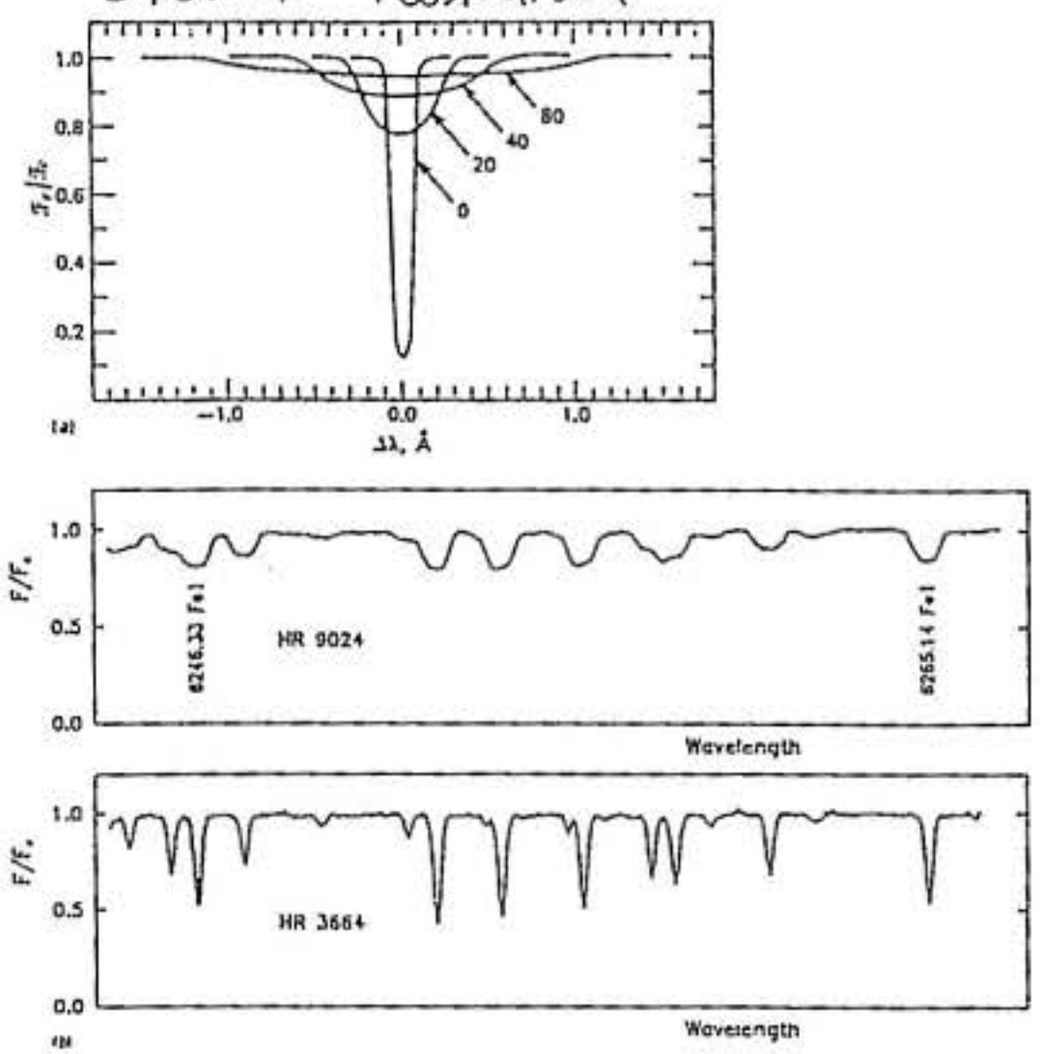

Fig. 17.7. (*a*) Computed profiles illustrate the broadening effect of rotation. The profiles are labeled with $\varepsilon \sin i$. the wavelength is 4243 Å. and the line has an equivalent width of 100 mÅ. (*b*) These two early-G giants illustrate the Doppler broadening of the line profiles by rotation.

Mass Loss

3

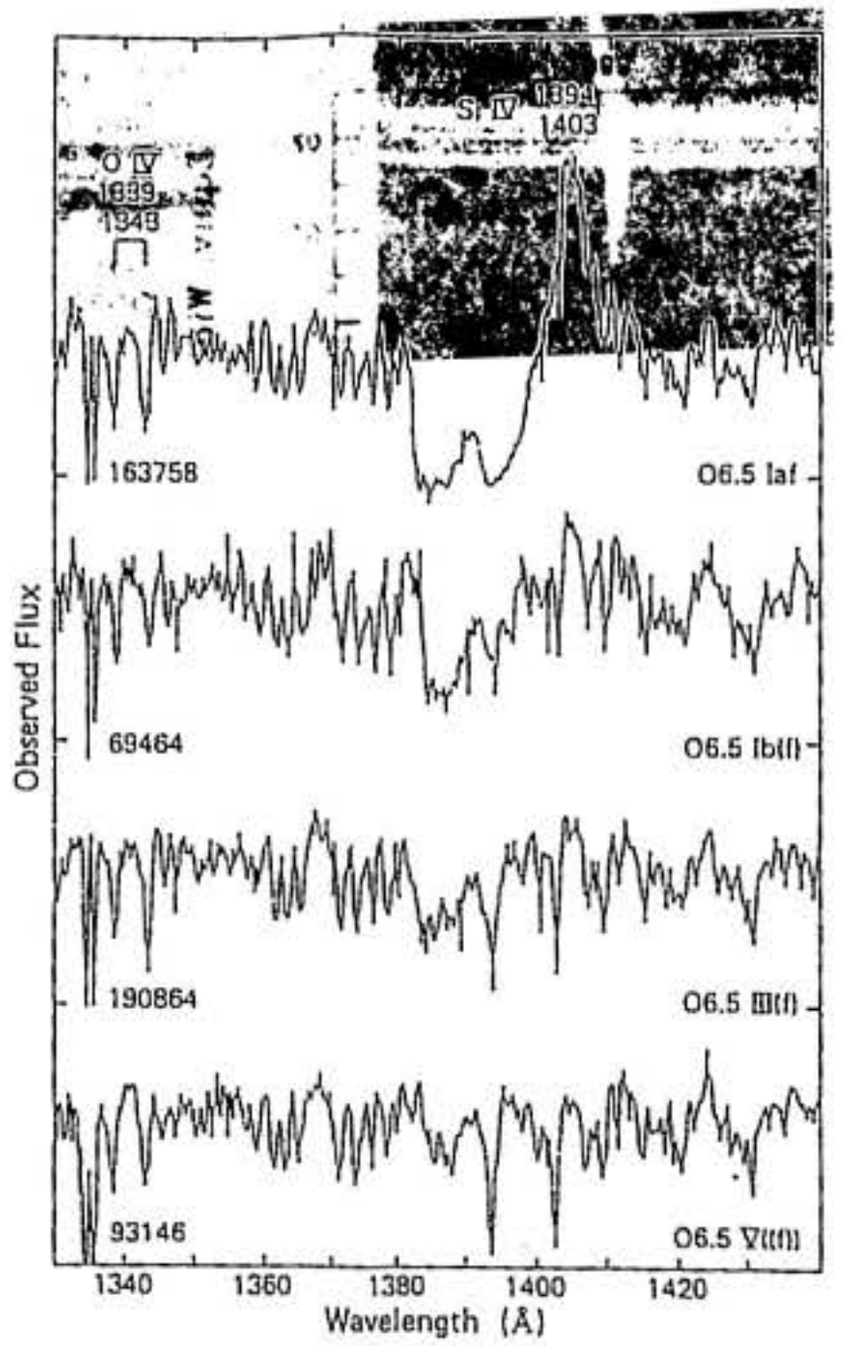

Figure 10.4. Si IV and stellar luminosity. The dwarf shows a pair of simple absorption lines. As we proceed to brighter stars, they strengthen, and in the supergiant, P Cygni emission-absorption features become very powerful. These lines show that an expanding envelope, or wind, develops toward higher luminosity. The spectra were taken with the International Ultraviolet Explorer (IUE) satellite operated by NASA. From an article in the *Astrophysical Journal*, by Nolan Walborn and Robert Panek.

Surface Mapping

4

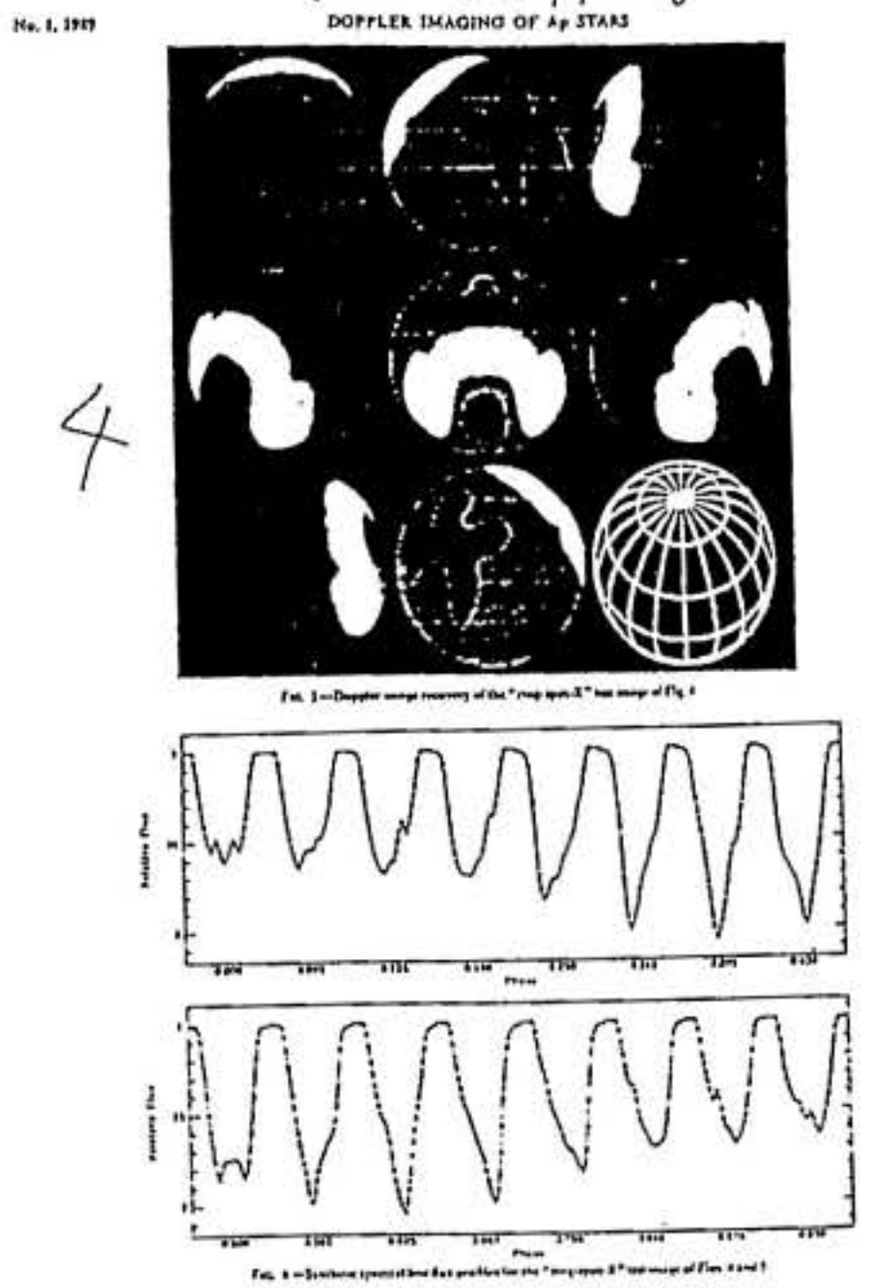

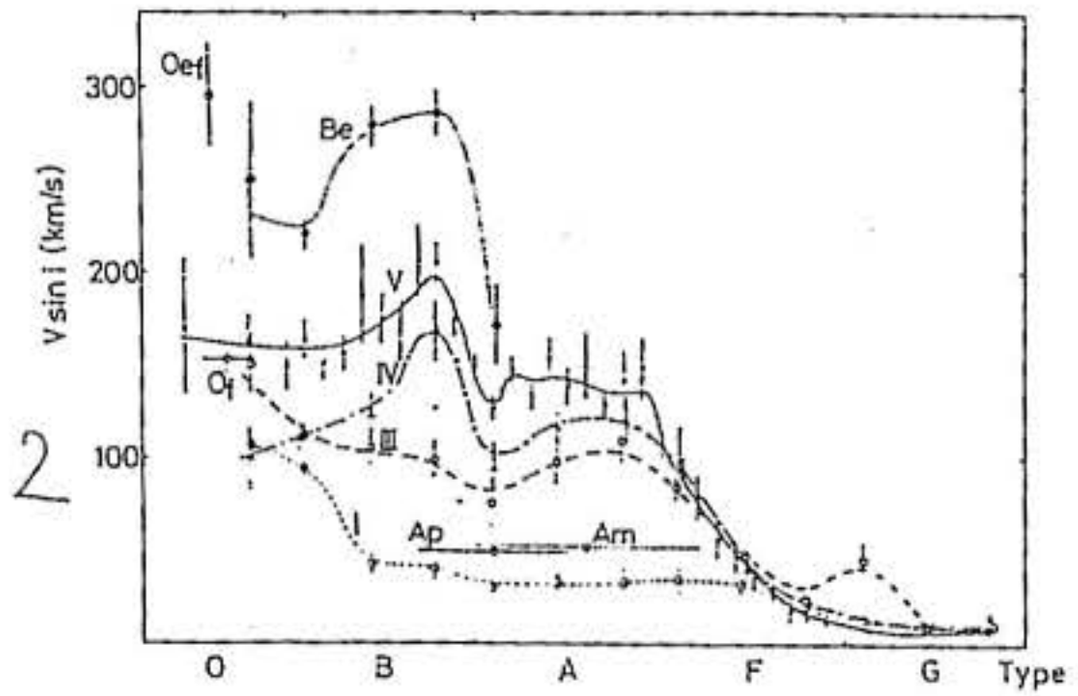

Figure 13.13. Distribution of Projected Stellar Rotational Velocities. The Roman numerals indicate the different luminosity classes. Some peculiar spectral types are indicated. The Of stars are O stars with emission features. Reproduced from *Publications of the Astronomical Society of the Pacific*, Vol. 94, p. 271 (1982). Courtesy of I. Fukuda.

2

5

6

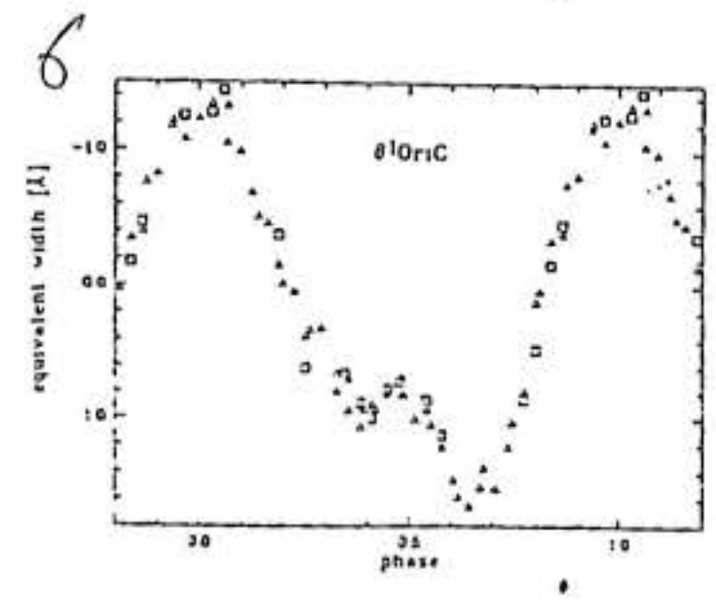

Fig. 3. Equivalent width of the Hα line of θ^1 Ori C versus phase (for an adopted period of 15.43 days and a zero point of MJD = 46832.5). Phase zero corresponds to maximum strength of the

星間吸収線

Spectral Information IV

オリオン座 δ 星

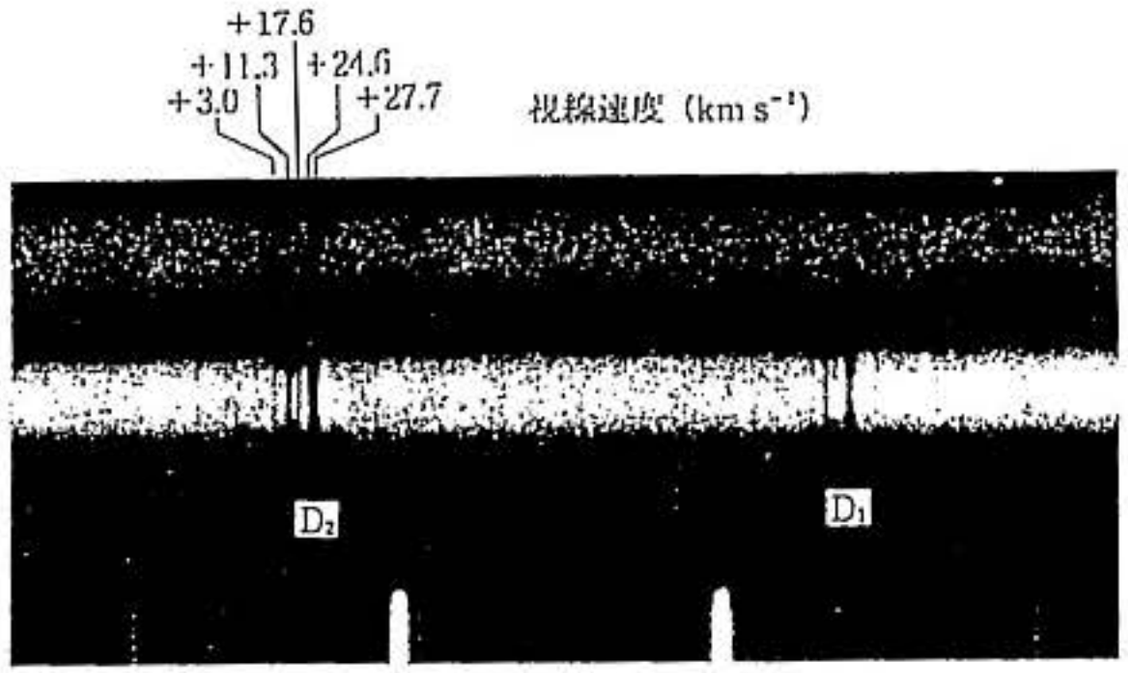

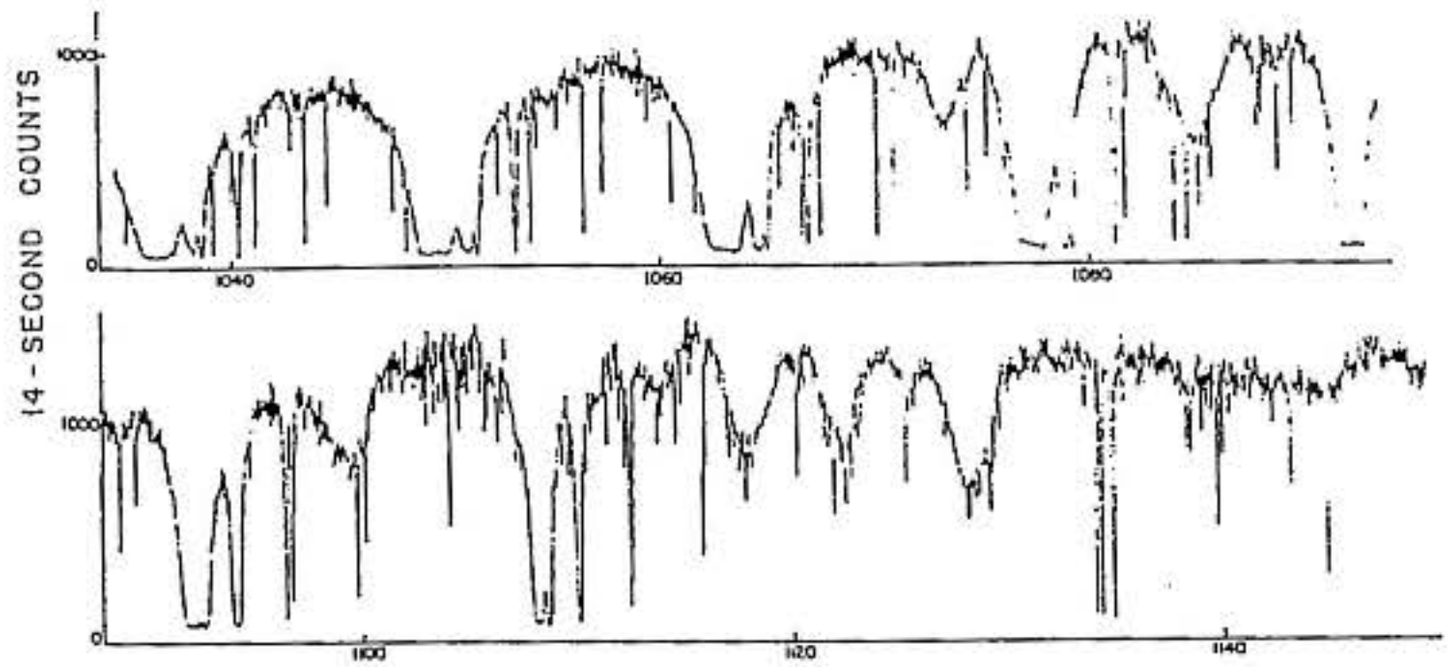

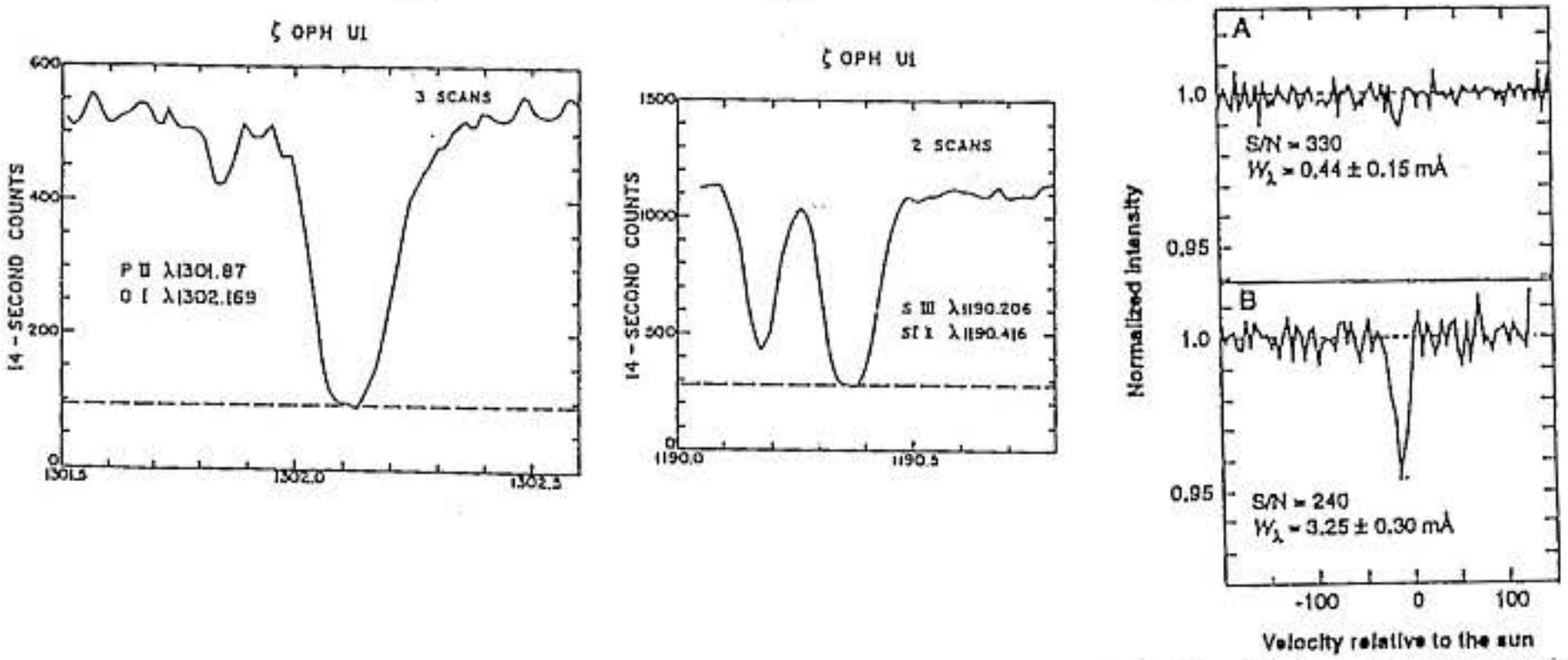

Fig. 1. Absorption lines of (A) Pb II λ 1433.9 Å and (B) Kr I λ 1235.8 Å observed in the spectrum of ζ Oph, plotted against the observed radial velocity (in kilometers per second) relative to the sun.

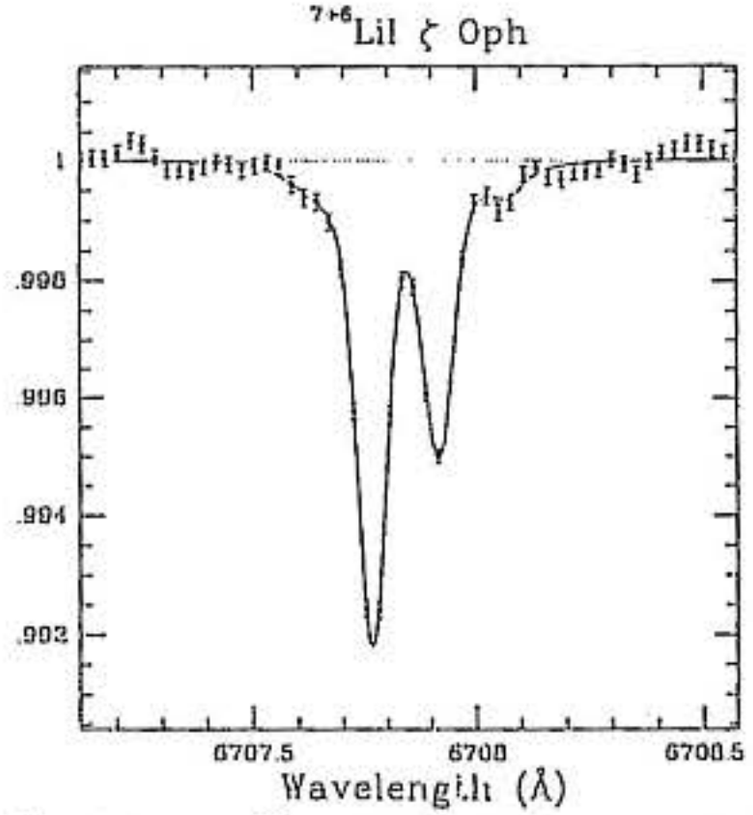

Figure 1: *Interstellar $^{6+7}$LiI absorption doublets toward ζ Oph. The data were gathered in June 1990 and June 1992 at ESO using the CES linked to the 3.6-m telescope via a fiber link. The total integration time is 15h., the resolution is $W/\Delta\lambda$ = 100,000, and the signal-to-noise ratio 7500 per pixel, or 11 per resolution element, giving a 3 σ limiting detectable equivalent width of 10 mÅ!*
The solid line represents the fit to the data with two interstellar absorbing clouds on the line of sight, and taking ^{6}Li and ^{7}Li absorptions into account. Ordinates are arbitrary units; error bars are 1 σ.

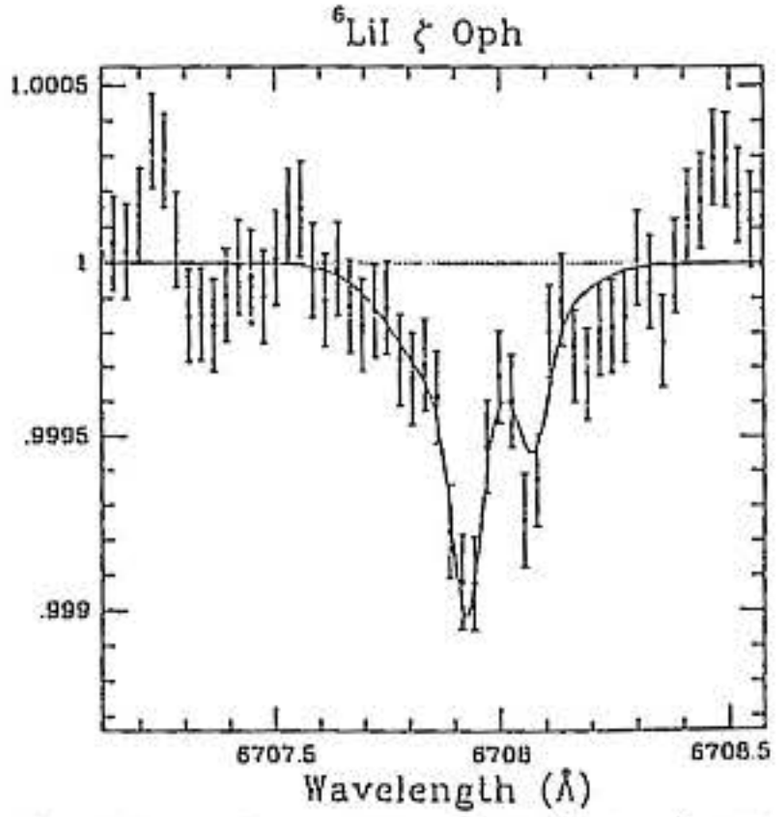

Figure 2: *Same as Figure 1, but the calculated ^{7}Li absorption was subtracted from the data points. These residuals thus reveal clearly the ^{6}Li absorption doublet. The depth of this doublet is less than 0.1 % of the continuum (see ordinates). The solid line represents the previously calculated ^{6}Li fit to this profile. Error bars are 1 σ.*

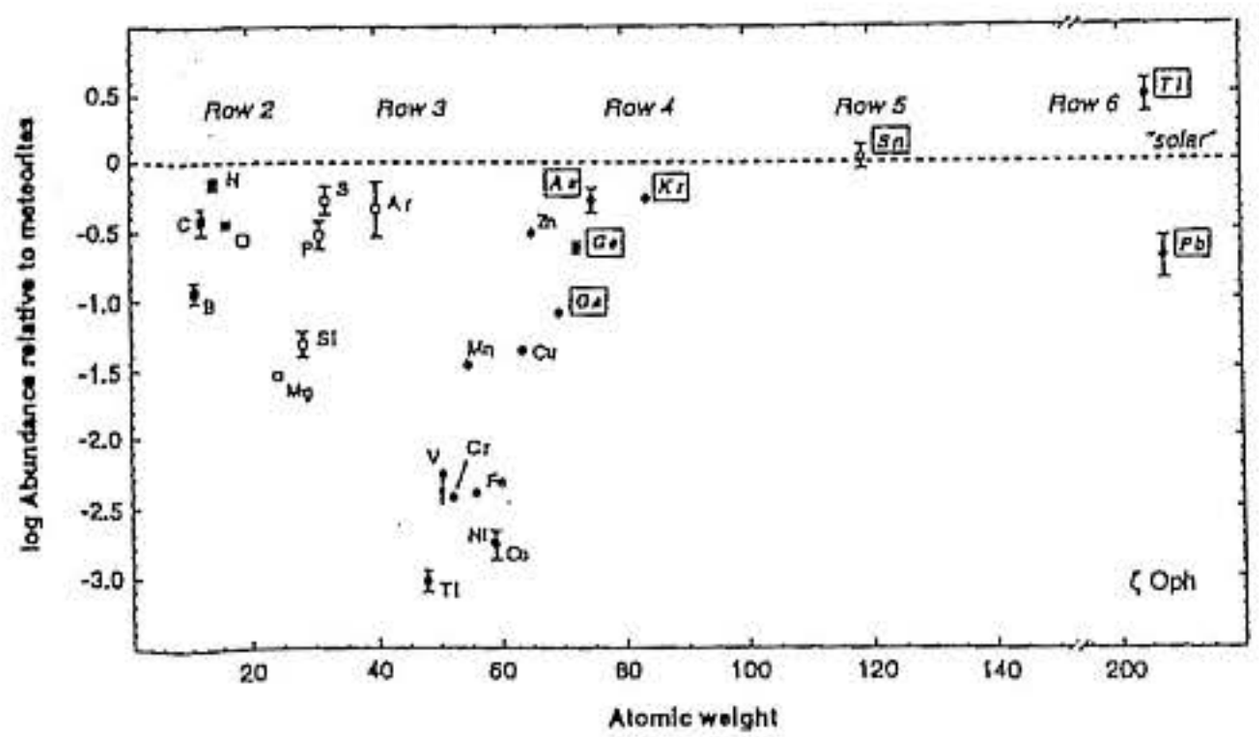

Fig. 2. The logarithm of the abundances of the heavy elements (boxed) observed toward ζ Oph (Table 1) relative to meteoritic (solar) abundances (3) plotted against mean atomic weight. For completeness we have also included data for the lighter elements. The specific rows in the periodic table in which these elements reside are also indicated and plotted with different symbols. The general deviation of different elements from the solar values is the result of their incorporation into dust.